DOI: 10.1002/ejic.200500898

A Systematic Exploration of Nickel(II)/Acetate/Di-2-pyridyl Ketone Chemistry: Neutral and Cationic Tetranuclear Clusters, and a Novel Mononuclear Complex

Constantinos G. Efthymiou,[a] Catherine P. Raptopoulou,[b] Aris Terzis,[b] Roman Boča,*[c] Maria Korabic,[d] Jerzy Mrozinski,*[d] Spyros P. Perlepes,*[a] and Evangelos G. Bakalbassis*[e]

Keywords: Acetate ligands / Di-2-pyridyl ketone / Magnetic properties / Nickel(II) cubanes / Nickel(II) defect dicubanes / X-ray diffraction

The further use of di-2-pyridyl ketone [$(2\text{-py})_2CO$] in nickel(II) acetate chemistry has been investigated. Various synthetic procedures have led to the synthesis of complexes $[Ni_4(O_2CMe)_2\{(2\text{-py})_2C(OH)O\}_4(H_2O)_2](ClO_4)_2$ (**1**), $[Ni(O_2CMe)\{(2\text{-py})_2C(OH)_2\}\{(2\text{-py})_2CO\}](ClO_4)\cdot H_2O$ (**2**·H_2O), $[Ni_4(O_2CMe)_3\{(2\text{-py})_2C(OH)O\}_4](ClO_4)\cdot 2H_2O\cdot 2EtOH$ (**3**·$2H_2O$·2EtOH), $[Ni_4(O_2CMe)_4\{(2\text{-py})_2C(OH)O\}_4]\cdot 2MeCN$ (**4**·2MeCN), and $[Ni_4(O_2CMe)_3\{(2\text{-py})_2C(OH)O\}_4](O_2CMe)\cdot 6H_2O\cdot MeCN$ (**5**·$6H_2O$·MeCN). The Ni^{II}-mediated hydrolysis of $(2\text{-py})_2CO$ to give the coordinated molecule $(2\text{-py})_2C(OH)_2$ or the monoanion $(2\text{-py})_2C(OH)O^-$ involves nucleophilic attack by H_2O on the carbonyl group. The Ni^{II} ion in **2**·H_2O is coordinated by one monodentate acetate, one *N*,*N*′,*O*-tridentate chelating $(2\text{-py})_2C(OH)_2$ molecule, and one *N*,*N*′-bidentate chelating $(2\text{-py})_2CO$ ligand. The tetranuclear cluster cation of **1** has a cubane $\{Ni_4(\mu_3\text{-}OR)_4\}^{4+}$ core with Ni^{II} ions and deprotonated oxygen atoms occupying alternate vertices. The $[Ni_4(O_2CMe)_3\{(2\text{-py})_2C(OH)O\}_4]^+$ cations present in the complexes **3**·$2H_2O$·2EtOH and **5**·$6H_2O$·MeCN have almost identical cubane structures that are different from the structure of the cation of **1**. The four metal ions in the centrosymmetric molecules of **4**·2MeCN are located at four vertices of a defect dicubane (with two missing vertices) and are bridged by six oxygen atoms. Characteristic IR bands are discussed in terms of the known structures of **1**–**5**. The magnetic data for the Ni^{II} cubane **1** has been modeled with two *J* values, and shows that the coupling consists of two ferromagnetically coupled pairs that are antiferromagnetically coupled to give a diamagnetic ground state. The magnetic properties of **4** have been modeled with three *J* values, and reveal competing antiferromagnetic and ferromagnetic coupling between the four Ni^{II} ions.

Introduction

The last 15 years have witnessed explosive growth in interest in the polynuclear complexes (clusters) of 3d-metals at intermediate oxidation states with primarily oxygen- and/or nitrogen-based ligation.[1] This has been mainly due to their relevance to two fields, bioinorganic chemistry[2] and molecular magnetic materials. For the latter field, the discovery that individual polynuclear molecules can function as nanoscale magnets was a significant development.[3,4] Such molecules have since been named single-molecule magnets (SMMs). Although Mn clusters at various oxidation levels have to date proven to be the most fruitful source of SMMs, complexes displaying SMM behavior are known for several other 3d-metals (e.g., V^{III}, Fe^{II}, Fe^{III}, Co^{II}, Ni^{II})[5] with various *S* values, both integer and half-integer. The future health of the field of 3d-metal clusters, and the chances of discovering high-spin molecules (molecules with a large *S*) and/or identifying new SMMs will benefit from the development of new synthetic routes for polynuclear complexes.

With the points mentioned above in mind, and in the context of "serendipitous assembly",[1b] our group[6] and others[7] have been exploring "ligand blend" reactions involving (i) the monoanion, $(2\text{-py})_2C(OH)O^-$, or the dianion, $(2\text{-py})_2CO_2^{2-}$, of the *gem*-diol form (derivative) of di-2-pyridyl ketone, $(2\text{-py})_2CO$, and carboxylates; and (ii) the monoanion, $(2\text{-py})_2C(OR)O^-$, of the hemiacetal form of $(2\text{-py})_2CO$ and carboxylates, with the belief that they might

[a] Department of Chemistry, University of Patras, 26504 Patras, Greece
E-mail: perlepes@patreas.upatras.gr
[b] Institute of Materials Science, NCSR "Demokritos", 15310 Aghia Paraskevi Attikis, Greece
[c] Department of Inorganic Chemistry, Slovak Technical University, 81237 Bratislava, Slovakia
E-mail: roman.boca@stuba.sk
[d] Institute of Chemistry, University of Wroclaw, 14 F. Joliot-Curie, 50383 Wroclaw, Poland
E-mail: jmroz@wchuwr.chem.uni.wrocl.pl
[e] Laboratory of Applied Quantum Chemistry, Department of Chemistry, Aristotle University of Thessaloniki, 54124 Thessaloniki, Greece
E-mail: bakalbas@chem.auth.gr

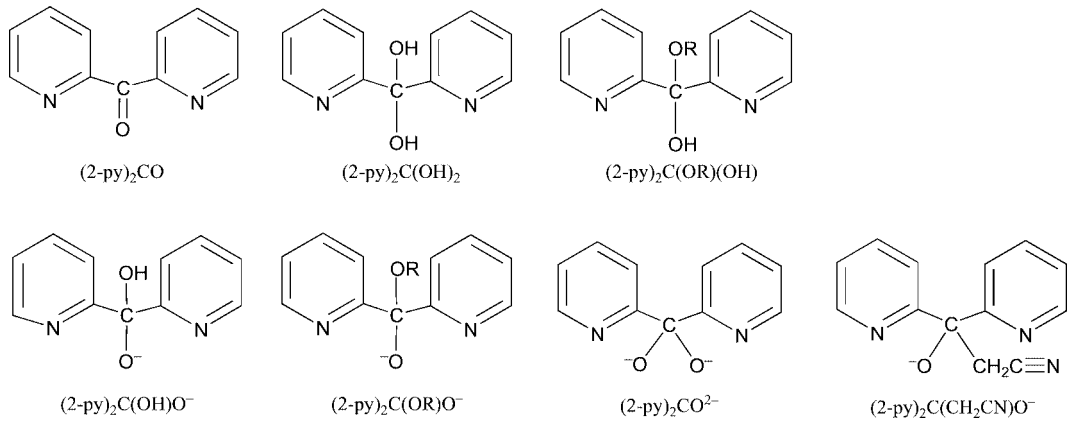

Figure 1. The formulae of the ligands discussed in the text; note that $(2\text{-py})_2C(OH)_2$, $(2\text{-py})_2C(OR)(OH)$, and all four anions do not exist as free species but exist only in their respective metal complexes.

foster the formation of discrete polynuclear metal systems. The formulae of these ligands are shown in Figure 1. The reactions of $(2\text{-py})_2CO$ with 3d-metal ions have been well studied over the years.[6–9] There is a chemical characteristic of $(2\text{-py})_2CO$ that makes this molecule a special ligand, this is its carbonyl group. Water and alcohols (ROH) have been shown to add to the carbonyl group upon coordination of the carbonyl oxygen atom and/or the 2-pyridyl rings forming the ligands $(2\text{-py})_2C(OH)_2$ [the *gem*-diol form of $(2\text{-py})_2CO$] and $(2\text{-py})_2C(OR)(OH)$ [the hemiacetal form of $(2\text{-py})_2CO$], respectively. The neutral ligands $(2\text{-py})_2C(OH)_2$ and $(2\text{-py})_2C(OR)(OH)$ coordinate to the metal centers as *N*,*N*′,*O* chelates, with the M–O bond often being weak; therefore, both neutral ligands do not hold much interest from the viewpoint of cluster formation.[8] Completely different and much more interesting (for cluster chemistry) coordination modes are seen when the ligands $(2\text{-py})_2C(OH)_2$ and $(2\text{-py})_2C(OR)(OH)$ are deprotonated. Upon deprotonation, the latter becomes monoanionic, while the former can function either as mono- or dianionic. The presence of deprotonated hydroxy group(s) leads to a great coordinative flexibility, because of the well-known ability of the negatively charged oxygen atom to bridge two or three metal ions. The monoanionic forms usually bridge two (μ_2) or three (μ_3) metal ions, while the dianionic form can bridge as many as five metal sites (μ_5). The immense structural diversity displayed by the complexes reported stems in part from the ability of $(2\text{-py})_2CO_2^{2-}$, $(2\text{-py})_2C(OH)O^-$, and $(2\text{-py})_2C(OR)O^-$ to exhibit no less than ten distinct coordination modes.[8] Carboxylates ($R'CO_2^-$) are employed for two reasons in the "ligand blends". Firstly, they are able to deprotonate the hydroxy group(s) under mild conditions (the use of external hydroxides often perplexes the reactions). Secondly, they are flexible ligands, a consequence of their ability to adopt a number of different ligation modes, both terminal and bridging as well as both bidentate and tridentate, giving an extraordinary structural versatility in the mixed-ligand systems. Thus, the $(2\text{-py})_2CO_2^{2-}/R'CO_2^-$, $(2\text{-py})_2C(OH)O^-/R'CO_2^-$, and $(2\text{-py})_2C(OR)O^-/R'CO_2^-$ "blends" (R = Me, Et; R′ = Me, CF_3, Ph), without (binary "blends") or with (ternary "blends") additional inorganic ligands [NO_3^-, N_3^-, SCN^-, $N(CN)_2^-$] have led to a variety of Mn, Fe, Co, Ni, and Cu clusters with nuclearities ranging from 3 to 14[8] and with interesting magnetic properties, including single-molecule magnetism.[6b]

Restricting further discussion to nickel(II) chemistry, the investigation of the binary $(2\text{-py})_2CO_2^{2-}$, $(2\text{-py})_2C(OH)O^-$, or $(2\text{-py})_2C(OR)O^-/MeCO_2^-$ "blend" has up to now led to clusters $[Ni_9(OH)_2(O_2CMe)_8\{(2\text{-py})_2CO_2\}_4]$,[6f] $[Ni_4(O_2CMe)_3\{(2\text{-py})_2C(OH)O\}_4](ClO_4)$,[7a] and $[Ni_4(O_2CMe)_4\{(2\text{-py})_2C(OH)O\}_4]$.[7b] We suspected that our,[6f] Tong's and Chen's,[7a] and Brown's and Krebs'[7b] groups had merely scratched the surface of this binary reaction system and we, thus, decided to perform a systematic synthetic study of the $Ni^{II}/MeCO_2^-/(2\text{-py})_2CO$ reaction system. Here we discuss the syntheses, structures, and IR spectra of the resulting products; the magnetic properties of two representative clusters will also be described and analyzed. The discovery of single-molecule magnetism in high-spin Ni^{II} cubane clusters[10] revived the interest in such compounds.

Results and Discussion

Synthesis

As stated above, we were interested in extending the very small family of $Ni^{II}/MeCO_2^-/(2\text{-py})_2CO$-based ligand complexes[6f,7a,7b] *without* the introduction of additional anionic inorganic ligands (binary "blends"). The chemical and structural identity of the products from the $Ni(O_2CMe)_2\cdot 4H_2O/(2\text{-py})CO$ reaction system depends on the solvent used, the presence/absence of counterions (this synthetic parameter is related to the choice of the solvent), the ligand–to-metal reaction ratio and the OH^- concentration. Our general route for the isolation of heteroleptic $(2\text{-py})_2CO_2^{2-}$, $(2\text{-py})_2C(OH)O^-$, or $(2\text{-py})_2C(OR)O^-/MeCO_2^-$ Ni^{II} clusters was to treat an excess of nickel(II) acetate with $(2\text{-py})_2CO$; we shall describe our efforts in terms of the solvent. Obviously "$(2\text{-py})_2C(OH)_2$" and "$(2\text{-py})_2C(OR)(OH)$" can be fully/partially deprotonated by the basic acetate groups and polynuclear $Ni^{II}/(2\text{-py})_2CO_2^{2-}$, $(2\text{-py})_2C(OH)O^-$, or $(2\text{-py})_2C(OR)O^-/MeCO_2^-$ complexes may result

$$4\ Ni(O_2CMe)_2{\cdot}4H_2O + 4\ (2\text{-py})_2CO + 2\ NaClO_4 \xrightarrow{H_2O} \underset{\mathbf{1}}{[Ni_4(O_2CMe)_2\{(2\text{-py})_2C(OH)O\}_4(H_2O)_2](ClO_4)_2} + 2\ NaO_2CMe + 4\ MeCO_2H + 10\ H_2O \quad (1)$$

from the reactions as long as the $MeCO_2^-$-to-$(2\text{-py})_2CO$ ratio is high enough to leave an amount of nonprotonated acetate in the reaction mixture, given the fact that the anionic forms of $(2\text{-py})_2CO$ and the acetate can adopt a variety of terminal and bridging modes.

Complexes **1** and **2** were prepared from aqueous reaction mixtures. The preparation of compound **1** can be achieved by the reaction of $Ni(O_2CMe)_2{\cdot}4H_2O$ with $(2\text{-py})_2CO$ according to the balanced Equation (1). One feature of the chemical Equation (1) deserves a comment.

This is the "wrong" stoichiometry, i.e. $Ni(O_2CMe)_2{\cdot}4H_2O/(2\text{-py})_2CO$ = 1.5:1, employed for the preparation of **1** (see Exp. Sect.) compared with that required by Equation (1) [1:1]. The "incorrect" reaction ratio is because of our desire to avoid the formation of the mononuclear complexes **2** and $[Ni\{(2\text{-py})_2C(OH)O\}\{(2\text{-py})_2C(OH)_2\}]_2[Ni\{(2\text{-py})_2C(OH)O\}_2](ClO_4)_2{\cdot}7H_2O$[11] that contain a 1:2 $Ni^{II}/(2\text{-py})_2CO$-based ligand ratio (vide infra). If we assume that the simplified chemical equilibrium represented by Equation (2) takes place (this is only one of the possible chemical equilibria), then the presence of an excess of nickel(II) acetate shifts the equilibrium to the right.

$$2\ [Ni(O_2CMe)\{(2\text{-py})_2C(OH)_2\}\{(2\text{-py})_2CO\}]^+ + 2\ Ni(O_2CMe)_2 + 4\ H_2O \rightleftharpoons [Ni_4(O_2CMe)_2\{(2\text{-py})_2C(OH)O\}_4(H_2O)_2]^{2+} + 4\ MeCO_2H \quad (2)$$

Having obtained and identified complex **1**, the next question addressed was whether, and in what manner, changes to the $Ni(O_2CMe)_2{\cdot}4H_2O/(2\text{-py})_2CO$ ratio might affect the product identity. In particular, we wondered whether it might be possible to prepare mononuclear complexes containing the ligand $(2\text{-py})_2C(OH)_2$ [the neutral *gem*-diol form of $(2\text{-py})_2CO$, Figure 1] and/or clusters containing the dianion $(2\text{-py})_2CO_2^{2-}$ [Figure 1] that are different from $[Ni_9(OH)_2(O_2CMe)_8\{(2\text{-py})_2CO_2\}_4]$ previously reported.[6f] We were successful with the first goal but unsuccessful with the second.

The 1:2 reaction between $Ni(O_2CMe)_2{\cdot}4H_2O$ and $(2\text{-py})_2CO$ in H_2O in the presence of an excess of $NaClO_4$ gave a mauve solution. Slow solvent evaporation at room temperature yielded crystals that were obviously a mixture of two products. Microscopic examination showed both brown-red prisms and mauve needles to be present in a visual ratio of roughly 3:1. The unit cell dimensions of hand-picked prisms and needles did not correspond to known compounds. Since repeated crystallizations from H_2O or H_2O/Me_2CO could not yield a sample free of the needles for elemental analysis, full data sets were collected for both compounds and the structures solved. The extreme differences in color and in crystal shape were fortuitous and allowed easy manual separation of the two materials. The prisms proved to be $[Ni(O_2CMe)\{(2\text{-py})_2C(OH)_2\}\{(2\text{-py})_2CO\}](ClO_4)$ (**2**) as its mono(water) solvate, while the needles were shown to be $[Ni\{(2\text{-py})_2C(OH)O\}\{(2\text{-py})_2C(OH)_2\}]_2[Ni\{(2\text{-py})_2C(OH)O\}_2](ClO_4)_2{\cdot}7H_2O$ consisting of two chemically similar cations, one neutral complex molecule, two perchlorate anions, and water solvate molecules.[11] The latter compound will not be further discussed because it will be incorporated into a full paper dealing with all the acetate-free complexes that have been isolated from the $Ni(O_2CMe)_2{\cdot}4H_2O/(2\text{-py})_2CO$ and $Ni(O_2CMe)_2{\cdot}4H_2O/(2\text{-py})_2CO/ClO_4^-$ reaction mixtures. The formation of **2** as an individual species can be summarized in the balanced Equation (3). With the identity of **2** established, we subsequently tried to devise a route to pure material. Complex **2** has a Ni^{II}/ClO_4^- ratio of 1:1, whereas the acetate-free complex has a Ni^{II}/ClO_4^- ratio of 3:2, i.e. 1.5:1. Thus, attempts to obtain pure **2** were made by further lowering the Ni^{II}/ClO_4^- ratio.

$$Ni(O_2CMe)_2{\cdot}4H_2O + 2\ (2\text{-py})_2CO + NaClO_4 \xrightarrow{H_2O} \underset{\mathbf{2}}{[Ni(O_2CMe)\{(2\text{-py})_2C(OH)_2\}\{(2\text{-py})_2CO\}](ClO_4)} + NaO_2CMe + 3\ H_2O \quad (3)$$

Somewhat to our disappointment, the use of Ni^{II}/ClO_4^- ratios of 1:2 or even of 1:3 again gave mixtures of **2** and $[Ni\{(2\text{-py})_2C(OH)O\}\{(2\text{-py})_2C(OH)_2\}]_2[Ni\{(2\text{-py})_2C(OH)O\}_2](ClO_4)_2{\cdot}7H_2O$. It is likely that the reaction solution contains a complicated mixture of several mononuclear species in equilibrium, with factors such as relative solubility, lattice energy, crystallization kinetics − amongst others − determining the identity of the isolated products.

The incorporation of a coordinated ligand molecule in its ketone form [$(2\text{-py})_2CO$] (Figure 1) in **2** was unexpected, given the fact that the complex was isolated from H_2O.[8] One possible reason for the presence of the $(2\text{-py})_2CO$ ligand is the satisfaction of the requirements of the crystal lattice. Another reason could be the combined tendencies of the acetate ion to coordinate (and not to act as a counterion) in the presence of ClO_4^- ions and of the Ni^{II} ion to adopt the octahedral stereochemistry; the monodentate acetate coordination (vide infra) "forces" the second neutral organic molecule to behave as a bidentate ligand; the bidentate chelating mode is much more common for $(2\text{-py})_2CO$ than for $(2\text{-py})_2C(OH)_2$.

The 3:1:1 or 2 $Ni(O_2CMe)_2{\cdot}4H_2O/(2\text{-py})_2CO/NaClO_4$ reaction mixtures in H_2O were also investigated due to our desire to doubly deprotonate the *gem*-diol form of $(2\text{-py})_2CO$ [as a consequence of the high $MeCO_2^-/(2\text{-py})_2C(OH)_2$ ratio] and to prepare complexes of $(2\text{-py})_2CO_2^{2-}$. However, such efforts were in vain. Complex **1** was again

isolated even employing a $Ni(O_2CMe)_2{\cdot}4H_2O/(2\text{-py})_2CO$ ratio of 4:1, emphasizing the fact that H_2O is not the appropriate solvent for the isolation of metal complexes of $(2\text{-py})_2CO_2^{2-}$.[6b,e,f,g,12]

The access to **1** and **2** from H_2O suggested that the reaction system might be capable of extension to other solvents. The 1:1 or 2:1 $Ni(O_2CMe)_2{\cdot}4H_2O/(2\text{-py})_2CO$ reaction mixtures in EtOH gave green crystals upon layering with Et_2O. The unit cell dimensions of a hand-picked crystal confirmed this product to be the known complex $[Ni_4(O_2CMe)_4\{(2\text{-py})_2C(OH)O\}_4]{\cdot}4EtOH$,[7b] on the basis of comparison with those of the authentic sample. We were rather surprised to see that this complex could not be easily isolated without the addition of Et_2O, e.g. upon slow solvent evaporation at room temperature. We suspected that a cationic species was present in solution and we thus reasoned that adding ClO_4^- ions might give a cationic cluster. Not only did the addition of ClO_4^- confirm our suspicion about the importance of the counterion in determining the reaction product but it also yielded a tetranuclear cluster with a topology (cubane) different from that of the neutral complex $[Ni_4(O_2CMe)_4\{(2\text{-py})_2C(OH)O\}_4]{\cdot}4EtOH$[7b] (defective double cubane). The formation of the tetranuclear cluster $[Ni_4(O_2CMe)_3\{(2\text{-py})_2C(OH)O\}_4](ClO_4)$ (**3**), which was crystallized upon lowering the temperature of the EtOH reaction solution can be summarized in the balanced Equation (4).

$$4\ Ni(O_2CMe)_2{\cdot}4H_2O + 4\ (2\text{-py})_2CO + NaClO_4 \xrightarrow{EtOH}$$

$$[Ni_4(O_2CMe)_3\{(2\text{-py})_2C(OH)O\}_4](ClO_4) + NaO_2CMe + 4\ MeCO_2H + 12\ H_2O \quad (4)$$

3

The "wrong" $Ni^{II}/(2\text{-py})_2CO/ClO_4^-$ ratio employed for the preparation of **3** (4:4:2, see Exp. Sect.) compared to that required by Equation (1) [4:4:1] did not prove detrimental to the formation of the complex. With the identity of **3** established, the "correct" stoichiometry was employed and led to the pure compound in high yield. The employment of EtOH as the solvent might imply the presence of the monoanion of the hemiacetal form of di-2-pyridyl ketone, i.e. $(2\text{-py})_2C(OEt)O^-$ (Figure 1) in the complex. However, only $(2\text{-py})_2C(OH)O^-$ ligands are present in complex **3**. It is difficult to rationalize this result; suffice it to say that the moisture present in solution (from the solvent and the starting materials) is responsible for the formation of the $(2\text{-py})_2C(OH)O^-$ ligands and that complex **3** is the thermodynamically stable product from the $Ni(O_2CMe)_2{\cdot}4H_2O/(2\text{-py})_2CO/NaClO_4$ reaction system in nonabsolute EtOH. It should be mentioned at this point that although the incorporation of $(2\text{-py})_2C(OMe)OH/(2\text{-py})_2C(OMe)O^-$ ligands in solid metal complexes isolated from MeOH is common,[8,9d,e,f,g,i,k,l,13] the participation of $(2\text{-py})_2C(OEt)OH/(2\text{-py})_2C(OEt)O^-$ ions in the coordination spheres of metal ions is rare[7b,9k] inspite of the plethora of reactions performed in EtOH.

The last reaction solvent investigated was *MeCN*. Previous synthetic studies on the $Ni(O_2CMe)_2{\cdot}4H_2O/(2\text{-py})_2CO/NaClO_4$ reaction system in $MeCN/H_2O$ (H_2O is necessary to keep the produced NaO_2CMe soluble) had led to the isolation of the cationic cubane cluster $[Ni_4(O_2CMe)_3\{(2\text{-py})_2C(OH)O\}_4](ClO_4)$.[7a] We wondered whether a neutral cluster could be formed in the absence of ClO_4^- ions. The 1:1 reaction between $Ni(O_2CMe)_2{\cdot}4H_2O$ and $(2\text{-py})_2CO$ in MeCN under reflux gave complex $[Ni_4(O_2CMe)_4\{(2\text{-py})_2C(OH)O\}_4]$ (**4**) in high yield according to the balanced Equation (5). We were happy to see (vide infra) that the structural motif in **4** (double defective cubane) is different from that in the cationic cluster isolated from the same solvent (cubane).[7a]

$$4\ Ni(O_2CMe)_2{\cdot}4H_2O + 4\ (2\text{-py})_2CO \xrightarrow[\Delta]{MeCN}$$

$$[Ni_4(O_2CMe)_4\{(2\text{-py})_2C(OH)O\}_4] + 4\ MeCO_2H + 12\ H_2O \quad (5)$$

4

The 2:1 and 3:1 reactions of $Ni(O_2CMe)_2{\cdot}4H_2O$ with $(2\text{-py})_2CO$ in MeCN under reflux gave a mixture of green crystals and green powder. The extreme difference in crystallinity was fortuitous and allowed ready manual separation of the two materials. The crystals were shown to be the known complex $[Ni_9(OH)_2(O_2CMe)_8\{(2\text{-py})_2CO_2\}_4]$[6f] by determination of the unit cell dimensions. The double deprotonation of the *gem*-diol form of di-2-pyridyl ketone is a consequence of the high $MeCO_2^-$ (base) to "$(2\text{-py})_2C(OH)_2$" ratio (4:1 or 6:1) used in the reactions. The green powder is certainly $Ni(O_2CMe)_2{\cdot}4H_2O$ (that was not initially dissolved), a conclusion consistent with IR data.

A last synthetic parameter that was studied was the OH^- concentration. Although it is well known that the use of external hydroxides often perplexes the reactions of metal ions with $(2\text{-py})_2CO$, we tried to prepare clusters containing $(2\text{-py})_2CO_2^{2-}$ ligands under conditions that favor formation of neutral or anionic complexes; for the latter purpose we employed bulky noncoordinating countercations, e.g. $NnBu_4^+$, BPh_4^+, and PPh_4^+. Synthetic studies of hundreds of $Ni(O_2CMe)_2{\cdot}4H_2O/(2\text{-py})_2CO/OH^-$ or $Ni(O_2CMe)_2{\cdot}4H_2O/(2\text{-py})_2CO/OH^-/Z^+$ (Z^+ = countercation) reaction systems in various solvents repeatedly led to amorphous or microcrystalline materials with poor analytical results. We were luckier when we employed a solvent mixture comprising EtOH and MeCN, and $LiOH{\cdot}H_2O$ as the base under reflux. Using a rather unusual crystallization process we isolated single crystals of complex $[Ni_4(O_2CMe)_3\{(2\text{-py})_2C(OH)O\}_4](O_2CMe)$ (**5**). However, we were unlucky at the same time because (i) the complex does not contain $(2\text{-py})_2CO_2^{2-}$ and (ii) the molecular structure of the cation is similar to that present in complex **3**. The formation of **5** can be summarized in the balanced Equation (6). The isolation of **5** that contains an acetate counterion was surprising and, needless to say, unexpected. Ethanol is necessary in the solvent mixture to keep $LiOH{\cdot}H_2O$ soluble, while treatment of the obtained residue (obtained after solvent evaporation under reduced pressure) with MeCN allows removal of the produced, insoluble

LiO_2CMe and dissolution of the cluster, which is subsequently crystallized pure upon storage of the resulting solution at 5 °C.

$$4\ Ni(O_2CMe)_2{\cdot}4H_2O + 4\ (2\text{-py})_2CO + 4\ LiOH{\cdot}H_2O \xrightarrow{EtOH/MeCN\ (3:1\ v/v)} [Ni_4(O_2CMe)_3\{(2\text{-py})_2C(OH)O\}_4](O_2CMe) + 4\ LiO_2CMe + 20\ H_2O \quad (6)$$

5

Description of Structures

[Ni(O$_2$CMe){(2-py)$_2$C(OH)$_2$}{(2-py)$_2$CO}](ClO$_4$)·H$_2$O (2·H$_2$O)

A partially labeled plot of the mononuclear cation $[Ni(O_2CMe)\{(2\text{-py})_2C(OH)_2\}\{(2\text{-py})_2CO\}]^+$ present in compound **2**·H_2O is shown in Figure 2. Selected bond lengths and angles are listed in Table 1. The structure consists of the above mentioned mononuclear cation, one ClO_4^- anion, and one H_2O solvate molecule.

Table 1. Selected bond lengths [Å] and angles [°] for [Ni(O$_2$CMe)-{(2-py)$_2$C(OH)$_2$}{(2-py)$_2$CO}](ClO$_4$)·H$_2$O (**2**·H$_2$O).

Ni–O(1)	2.157(2)	C(6)–O(1)	1.417(5)
Ni–O(3)	2.045(3)	C(6)–O(2)	1.387(4)
Ni–N(1)	2.085(3)	C(26)–O(11)	1.218(5)
Ni–N(2)	2.094(3)	C(41)–O(3)	1.248(5)
Ni–N(11)	2.038(3)	C(41)–O(4)	1.266(5)
Ni–N(12)	2.060(3)		
O(1)–Ni–O(3)	94.7(1)	O(3)–Ni–N(12)	89.6(1)
O(1)–Ni–N(1)	76.4(1)	N(1)–Ni–N(2)	88.0(1)
O(1)–Ni–N(2)	77.0(1)	N(1)–Ni–N(11)	98.0(1)
O(1)–Ni–N(11)	173.0(1)	N(1)–Ni–N(12)	94.3(1)
O(1)–Ni–N(12)	95.0(1)	N(2)–Ni–N(11)	98.7(1)
O(3)–Ni–N(1)	171.1(1)	N(2)–Ni–N(12)	170.9(1)
O(3)–Ni–N(2)	89.8(1)	N(11)–Ni–N(12)	89.7(1)
O(3)–Ni–N(11)	90.9(1)		

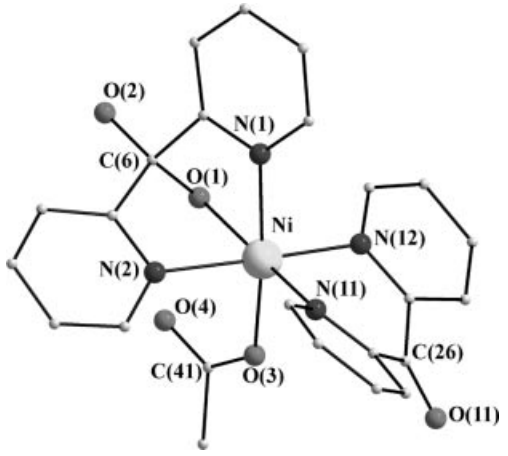

Figure 2. Partially labeled ORTEP plot of the mononuclear cation present in complex **2**·H_2O.

The Ni^{II} atom is coordinated by one monodentate acetate, one tridentate chelating $(2\text{-py})_2C(OH)_2$ molecule, and one bidentate chelating $(2\text{-py})_2CO$ ligand. The ligated atoms of the latter are the 2-pyridyl nitrogen atoms (Figure 3), while the *gem*-diol ligand adopts the coordination mode $\eta^1{:}\eta^1{:}\eta^1$, see also Figure 3. The two oxygen atoms [O(1), O(3)] are in *cis* positions. The Ni–N and Ni–O bond lengths agree well with values expected for high-spin Ni^{II} in octahedral environments.[7a,b,10] The distortion from a perfect octahedral geometry is primarily a consequence of the presence of three different ligands in the coordination sphere of Ni^{II}. The short length of the C(26)–O(11) bond [1.218(5) Å, compared with the C(6)–O(1, 2) bond lengths of 1.387(4) and 1.417(5) Å] reflects the ketone character of this group. There is one strong intramolecular hydrogen bond with the coordinated hydroxy oxygen of $(2\text{-py})_2C(OH)_2$ as the donor and the uncoordinated acetate oxygen

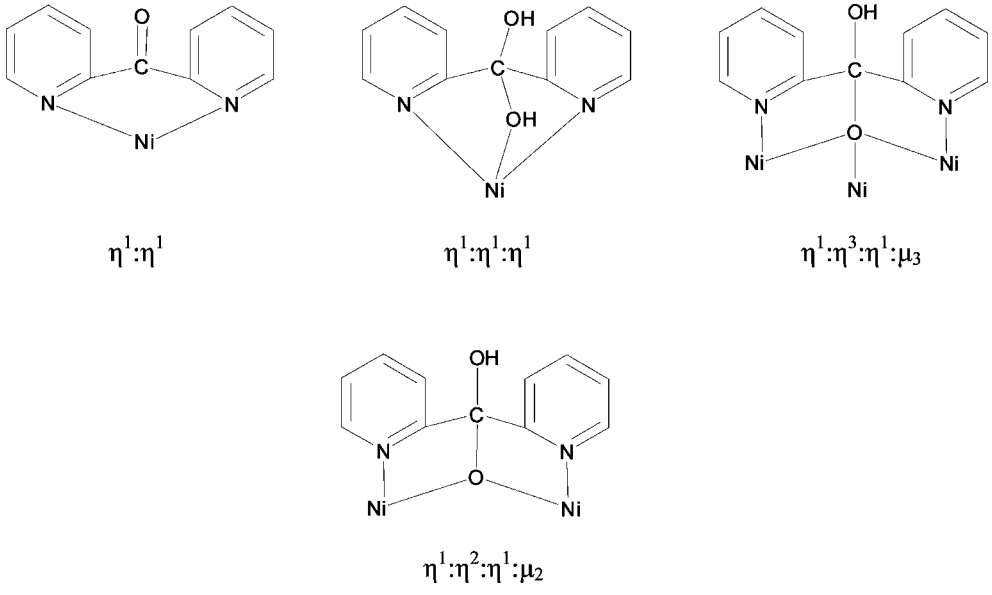

$\eta^1{:}\eta^1$ $\eta^1{:}\eta^1{:}\eta^1$ $\eta^1{:}\eta^3{:}\eta^1{:}\mu_3$

$\eta^1{:}\eta^2{:}\eta^1{:}\mu_2$

Figure 3. The crystallographically established coordination modes of the ligands $(2\text{-py})_2CO$, $(2\text{-py})_2C(OH)_2$, and $(py)_2C(OH)O^-$ present in complexes **1**–**5**.

as the acceptor; its dimensions are: O(1)···O(4) 2.525 Å, H(O1)···O(4) 1.688 Å, and O(1)–H(O1)···O(4) 168.7°. The crystal structure is stabilized by a hydrogen bond in which the uncoordinated hydroxy oxygen of the *gem*-diol ligand acts as the donor and one of the perchlorate oxygen atoms as the acceptor; the corresponding dimensions are O(2)···O(7) [$-x$, $y - 1/2$, $-z + 1$] 2.700 Å, H(O2)···O(7) 1.828 Å, and O(2)–H(O2)···O(7) 161.8°.

Compound **2**·H_2O is the first example of a metal complex in which the ketone [$(2\text{-py})_2CO$] and the *gem*-diol [$(2\text{-py})_2C(OH)_2$] forms of di-2-pyridyl ketone co-exist as ligands.

[$Ni_4(O_2CMe)_2\{(2\text{-py})_2C(OH)O\}_4(H_2O)_2$](ClO$_4$)$_2$ (1), [$Ni_4(O_2CMe)_3\{(2\text{-py})_2C(OH)O\}_4$](ClO$_4$)·2H$_2$O·2EtOH (3·2H$_2$O·2EtOH), and [$Ni_4(O_2CMe)_3\{(2\text{-py})_2$-$C(OH)O\}_4$]($O_2$CMe)·6H$_2$O·MeCN (5·6H$_2$O·MeCN)

Partially labeled plots of the tetranuclear cations present in compounds **1**, **3**·2H_2O·2EtOH, and **5**·6H_2O·MeCN are shown in Figure 4, Figure 5, and Figure 6, respectively. Tables 2, 3, 4, 5, and 6 show selected interatomic distances plus angles and hydrogen bonding data for complexes **1** and **5**·6H_2O·MeCN.

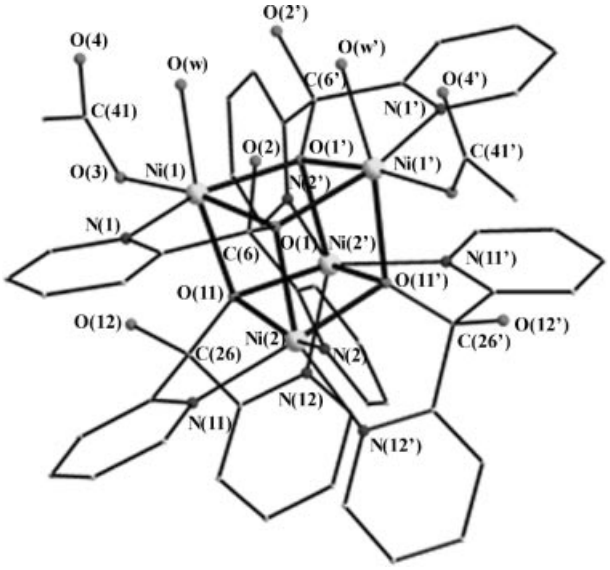

Figure 4. Partially labeled ORTEP plot of the tetranuclear cation present in complex **1**. Primed and unprimed atoms are related by the crystallographic twofold axis.

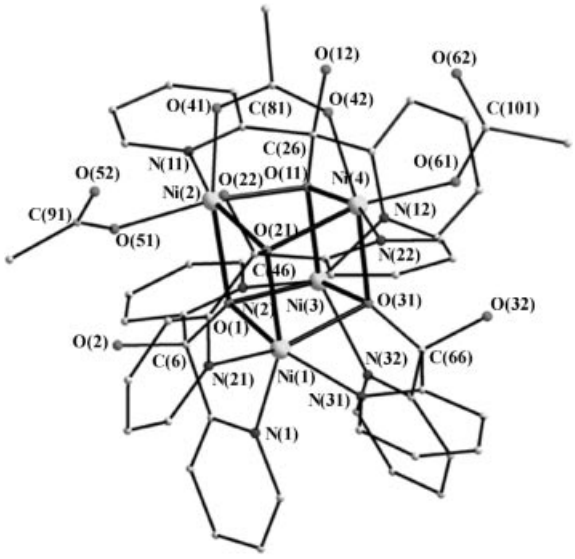

Figure 5. Partially labeled ORTEP plot of the tetranuclear cation present in complex **3**·2H_2O·2EtOH. The cubane core is outlined in bold.

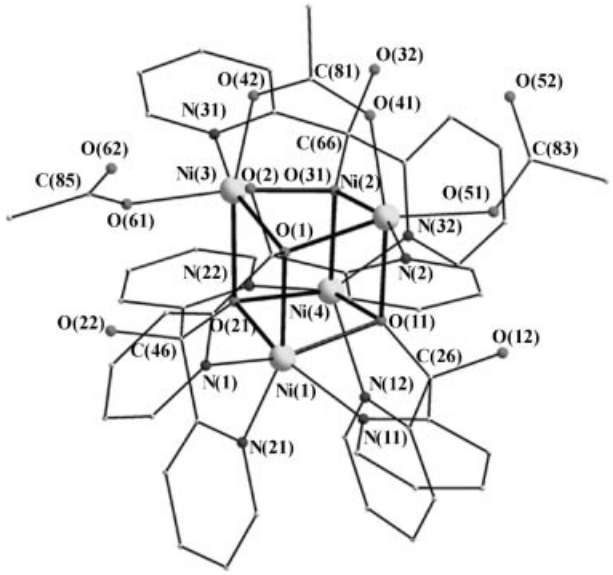

Figure 6. Partially labeled ORTEP plot of the tetranuclear cation present in complex **5**·6H_2O·MeCN. The cubane core is outlined in bold.

Complex **1** crystallizes in monoclinic space group *C*2/*c*. Its structure consists of tetranuclear [$Ni_4(O_2CMe)_2\{(2\text{-py})_2$-$C(OH)O\}_4(H_2O)_2$]$^{2+}$ cations and well-separated ClO_4^- counterions; the latter will not be further discussed. The tetranuclear cluster cation of **1** lies on a crystallographic twofold axis and has a cubane $\{Ni_4(\mu_3\text{-}OR)_4\}^{4+}$ core with Ni^{II} and oxygen atoms occupying alternate vertices. In addition to three μ_3-oxygen atoms, each of the metal ions Ni(1) and Ni(1′) is coordinated to one pyridyl N atom, to one aquo ligand, and to one O atom from a monodentate acetate ligand, whereas each of Ni(2) and Ni(2′) is coordinated to three pyridyl N atoms belonging to different $(2\text{-py})_2C(OH)O^-$ ligands. Thus, an octahedral coordination environment is created about each metal center; the chromophores are Ni(1, 1′)O_5N and Ni(2, 2′)O_3N_3. One octahedral face of each Ni^{II} atom is occupied by the three alkoxide-type oxygen atoms and the other contains the remaining donor atoms.

One oxygen atom [O(2), O(2′), O(12), O(12′)] of each $(2\text{-py})_2C(OH)O^-$ ligand remains protonated and unbound to the metal ions. The resultant monoanion functions as a $\eta^1{:}\eta^3{:}\eta^1{:}\mu_3$ ligand (Figure 3). This ligation mode is common for $(2\text{-py})_2C(OH)O^-$.[8]

There are two types of Ni–O (alkoxide-type) bonds for each metal ion: one bond is rather short at an average dis-

Table 2. Selected interatomic distances [Å] and angles [°] for $[Ni_4(O_2CMe)_2\{(2\text{-py})_2C(OH)O\}_4(H_2O)_2](ClO_4)_2$ (**1**).[a]

Ni(1)···Ni(2)	3.157(1)	Ni(2)–O(1)	2.122(3)
Ni(1)···Ni(2′)	3.272(1)	Ni(2)–O(11)	2.111(3)
Ni(1)···Ni(1′)	3.139(1)	Ni(2)–O(11′)	2.034(3)
Ni(2)···Ni(2′)	3.060(1)	Ni(2)–N(2)	2.036(4)
Ni(1)–O(1)	2.030(3)	Ni(2)–N(11)	2.095(4)
Ni(1)–O(1′)	2.133(3)	Ni(2)–N(12′)	2.085(4)
Ni(1)–O(3)	2.013(4)	C(41)–O(3)	1.277(6)
Ni(1)–O(11)	2.117(3)	C(41)–O(4)	1.229(8)
Ni(1)–O(w)	2.072(5)	C(6)–O(1)	1.390(6)
Ni(1)–N(1)	2.083(4)	C(6)–O(2)	1.410(7)
O(1)–Ni(1)–O(1′)	80.6(1)	O(1)–Ni(2)–N(11)	109.0(2)
O(1)–Ni(1)–O(3)	171.0(1)	O(1)–Ni(2)–N(12′)	155.1(2)
O(1)–Ni(1)–O(11)	82.1(1)	O(11)–Ni(2)–O(11′)	83.2(1)
O(1)–Ni(1)–O(w)	94.7(2)	O(11)–Ni(2)–N(2)	154.7(2)
O(1)–Ni(1)–N(1)	78.2(2)	O(11)–Ni(2)–N(11)	77.1(2)
O(1′)–Ni(1)–O(3)	99.6(2)	O(11)–Ni(2)–N(12′)	106.7(1)
O(1′)–Ni(1)–O(11)	76.6(1)	O(11′)–Ni(2)–N(2)	104.9(2)
O(1′)–Ni(1)–O(w)	92.7(2)	O(11′)–Ni(2)–N(11)	157.0(2)
O(1′)–Ni(1)–N(1)	158.8(2)	O(11′)–Ni(2)–N(12′)	74.5(2)
O(3)–Ni(1)–O(11)	89.2(1)	N(2)–Ni(2)–N(11)	98.0(2)
O(3)–Ni(1)–O(w)	94.3(2)	N(2)–Ni(2)–N(12′)	98.5(2)
O(3)–Ni(1)–N(1)	101.3(2)	N(11)–Ni(2)–N(12′)	95.9(2)
O(11)–Ni(1)–O(w)	169.2(2)	Ni(1)–O(1)–Ni(1′)	97.9(1)
O(11)–Ni(1)–N(1)	100.4(2)	Ni(1)–O(1)–Ni(2)	99.0(1)
O(w)–Ni(1)–N(1)	89.0(2)	Ni(1)–O(11)–Ni(2)	96.6(1)
O(1)–Ni(2)–O(11)	80.1(2)	Ni(1)–O(11)–Ni(2′)	104.0(1)
O(1)–Ni(2)–O(11′)	78.6(1)	Ni(1′)–O(1)–Ni(2)	100.6(1)
O(1)–Ni(2)–N(2)	78.1(2)	Ni(2)–O(11)–Ni(2′)	95.2(1)

[a] Primed atoms are related to the unprimed ones by the symmetry transformation $-x + 1$, y, $-z + 1/2$.

Table 3. Details for the hydrogen bonding of complex $[Ni_4(O_2CMe)_2\{(2\text{-py})_2C(OH)O\}_4(H_2O)_2](ClO_4)_2$ (**1**).[a]

D–H···A	D···A [Å]	H···A [Å]	DHA [°]	Symmetry operator of A
O(w)–H(wA)···O(4)[b]	2.670	1.990	171.8	x, y, z
O(w)–H(wB)···O(2′)[b]	2.997	2.495	122.4	$-x + 1$, y, $-z + 1/2$
O(12)–H(O12)···O(3)[b]	2.698	2.012	177.2	x, y, z
O(2)–H(O2)···O(7)[c]	3.096	2.521	176.1	$-x + 1/2$, $y + 1/2$, $-z + 1/2$

[a] A = acceptor; D = donor. [b] Intramolecular hydrogen bonds. [c] O(7) is a perchlorate oxygen atom.

tance of 2.032(3) Å, whereas the two other bonds are longer [average distance 2.121(3) Å]. The cube deviates from the ideal geometry. The internal cube angles (RO–Ni–OR) at the metal vertices average 80.2(2)°, whereas the corresponding angles at the alkoxide corners (Ni–OR–Ni) are much larger averaging 98.9(1)°. The Ni···Ni vectors in the cluster reflect the different Ni–O (alkoxide-type) bond lengths, with the Ni(1)···Ni(2′)/Ni(1′)···Ni(2) [3.272(1) Å] and Ni(2)···Ni(2′) [3.060(1) Å] distances being the longest and the shortest, respectively. The shortest Ni···Ni distance corresponds to the smallest Ni–O–Ni [95.2(1)°] and the largest O–Ni–O [83.2(1)°] internal cube angles, whereas the longest Ni···Ni distance corresponds to the larger Ni–O–Ni [average 102.3(1)°] and the smaller O–Ni–O [average 77.6(1)°] angles. Average Ni–N, Ni–O (alkoxide-type), and Ni–O (acetate) bond lengths of 2.075(4), 2.091(3), and 2.013(4) Å, respectively, lie well within the range of reported

Table 4. Selected interatomic distances [Å] and angles [°] for $[Ni_4(O_2CMe)_3\{(2\text{-py})_2C(OH)O\}_4](ClO_4)\cdot 2H_2O\cdot 2EtOH$ (**3**·$2H_2O$·2EtOH).

Ni(1)···Ni(2)	3.258(2)	Ni(3)–O(1)	2.106(6)
Ni(1)···Ni(3)	3.038(2)	Ni(3)–O(11)	2.100(7)
Ni(1)···Ni(4)	3.173(2)	Ni(3)–O(31)	2.045(7)
Ni(2)···Ni(3)	3.195(2)	Ni(3)–N(2)	2.084(9)
Ni(2)···Ni(4)	2.970(2)	Ni(3)–N(12)	2.058(9)
Ni(3)···Ni(4)	3.286(2)	Ni(3)–N(32)	2.103(9)
Ni(1)–O(1)	2.025(6)	Ni(4)–O(11)	2.092(6)
Ni(1)–O(21)	2.075(6)	Ni(4)–O(21)	2.044(6)
Ni(1)–O(31)	2.105(7)	Ni(4)–O(31)	2.201(7)
Ni(1)–N(1)	2.088(8)	Ni(4)–O(42)	2.016(8)
Ni(1)–N(21)	2.043(9)	Ni(4)–O(61)	1.993(9)
Ni(1)–N(31)	2.079(9)	Ni(4)–N(22)	2.085(9)
Ni(2)–O(1)	2.162(6)	C(101)–O(61)	1.25(2)
Ni(2)–O(11)	2.037(7)	C(101)–O(62)	1.23(2)
Ni(2)–O(21)	2.099(7)	C(91)–O(51)	1.269(14)
Ni(2)–O(41)	2.021(8)	C(91)–O(52)	1.234(14)
Ni(2)–O(51)	2.030(7)	C(81)–O(41)	1.277(15)
Ni(2)–N(11)	2.079(9)	C(81)–O(42)	1.220(15)
O(1)–Ni(1)–N(31)	158.6(3)	Ni(1)–O(1)–Ni(2)	102.1(3)
O(21)–Ni(1)–N(1)	154.9(3)	Ni(1)–O(1)–Ni(3)	94.7(3)
O(31)–Ni(1)–N(21)	155.7(3)	Ni(1)–O(21)–Ni(2)	102.6(3)
O(1)–Ni(2)–O(41)	167.2(3)	Ni(1)–O(21)–Ni(4)	100.8(3)
O(11)–Ni(2)–O(51)	166.2(3)	Ni(1)–O(31)–Ni(3)	94.1(3)
O(21)–Ni(2)–N(11)	162.2(3)	Ni(1)–O(31)–Ni(4)	94.9(3)
O(1)–Ni(3)–N(12)	154.4(3)	Ni(2)–O(1)–Ni(3)	96.9(2)
O(11)–Ni(3)–N(32)	154.3(3)	Ni(2)–O(11)–Ni(3)	101.1(3)
O(31)–Ni(3)–N(2)	156.9(3)	Ni(2)–O(11)–Ni(4)	92.0(3)
O(11)–Ni(4)–N(22)	162.6(3)	Ni(2)–O(21)–Ni(4)	91.6(3)
O(21)–Ni(4)–O(61)	166.9(4)	Ni(3)–O(11)–Ni(4)	103.2(3)
O(31)–Ni(4)–O(42)	166.2(3)	Ni(3)–O(31)–Ni(4)	101.4(3)

Table 5. Selected interatomic distances [Å] and angles [°] for $[Ni_4(O_2CMe)_3\{(2\text{-py})_2C(OH)O\}_4](O_2CMe)\cdot 6H_2O\cdot MeCN$ (**5**·$6H_2O$·MeCN).

Ni(1)···Ni(2)	3.189(1)	Ni(3)–O(1)	2.112(2)
Ni(1)···Ni(3)	3.267(1)	Ni(3)–O(21)	2.173(2)
Ni(1)···Ni(4)	3.026(1)	Ni(3)–O(31)	2.052(2)
Ni(2)···Ni(3)	2.976(1)	Ni(3)–O(42)	2.009(3)
Ni(2)···Ni(4)	3.285(1)	Ni(3)–O(61)	2.012(3)
Ni(3)···Ni(4)	3.178(1)	Ni(3)–N(31)	2.073(3)
Ni(1)–O(1)	2.076(2)	Ni(4)–O(11)	2.039(2)
Ni(1)–O(11)	2.117(2)	Ni(4)–O(21)	2.083(2)
Ni(1)–O(21)	2.026(2)	Ni(4)–O(31)	2.085(2)
Ni(1)–N(1)	2.028(3)	Ni(4)–N(12)	2.087(3)
Ni(1)–N(11)	2.089(3)	Ni(4)–N(22)	2.087(3)
Ni(1)–N(21)	2.077(3)	Ni(4)–N(32)	2.038(3)
Ni(2)–O(1)	2.040(2)	C(81)–O(41)	1.268(4)
Ni(2)–O(11)	2.175(2)	C(81)–O(42)	1.251(4)
Ni(2)–O(31)	2.097(2)	C(83)–O(51)	1.280(4)
Ni(2)–O(41)	2.020(2)	C(83)–O(52)	1.221(5)
Ni(2)–O(51)	2.043(2)	C(85)–O(61)	1.282(5)
Ni(2)–N(2)	2.088(3)	C(85)–O(62)	1.219(5)
O(1)–Ni(1)–N(21)	155.5(1)	Ni(1)–O(1)–Ni(2)	101.6(1)
O(11)–Ni(1)–N(1)	155.4(1)	Ni(1)–O(1)–Ni(3)	102.5(1)
O(21)–Ni(1)–N(11)	157.4(1)	Ni(1)–O(11)–Ni(2)	96.0(1)
O(1)–Ni(2)–O(51)	164.4(1)	Ni(1)–O(11)–Ni(4)	93.4(1)
O(11)–Ni(2)–O(41)	166.5(1)	Ni(1)–O(21)–Ni(3)	102.1(1)
O(31)–Ni(2)–N(2)	162.3(1)	Ni(1)–O(21)–Ni(4)	94.8(1)
O(1)–Ni(3)–N(31)	162.0(1)	Ni(2)–O(1)–Ni(3)	91.6(1)
O(21)–Ni(3)–O(42)	166.0(1)	Ni(2)–O(11)–Ni(4)	102.4(1)
O(31)–Ni(3)–O(61)	165.5(1)	Ni(2)–O(31)–Ni(3)	91.6(1)
O(11)–Ni(4)–N(22)	158.6(1)	Ni(2)–O(31)–Ni(4)	103.6(1)
O(21)–Ni(4)–N(32)	155.5(1)	Ni(3)–O(21)–Ni(4)	96.6(1)
O(31)–Ni(4)–N(12)	154.9(1)	Ni(3)–O(31)–Ni(4)	100.4(1)

Table 6. Established and possible hydrogen bonds for $[Ni_4(O_2CMe)_3\{(2\text{-py})_2C(OH)O\}_4](O_2CMe)\cdot 6H_2O\cdot MeCN$ (**5**·$6H_2O$·MeCN).[a]

D–H···A	D···A [Å]	H···A [°]	DHA [°]	Symmetry operator of A
O(2)–H(O2)···O(62)	2.710	1.945	169.8	*x*, *y*, *z*
O(12)–H(O12)···O(51)	2.718	1.981	167.0	*x*, *y*, *z*
O(22)–H(O22)···O(61)	2.716	1.975	166.0	*x*, *y*, *z*
O(32)–H(O32)···O(52)	2.666	1.974	162.3	*x*, *y*, *z*
O(W1)–H(OW1A)···O(W6)	2.720	1.969	161.3	*x*, *y*, *z*
O(W1)–H(OW1B)···O(62)	2.900	1.951	163.5	*x*, *y*, *z*
O(W2)–H(OW2A)···O(71)[b]	2.628	1.614	154.4	–*x* + 1, –*y* + 1, –*z* + 1
O(W2)–H(OW2B)···O(W3)	2.451	1.625	157.4	–*x*, –*y* + 1, –*z* + 1
O(W3)···O(W4)	2.526			–*x*, –*y* + 1, –*z* + 1
O(W3)···O(W3)	2.863			–*x*, –*y* + 1, –*z* + 1
O(W4)···O(72)[b]	2.388			–*x* + 1, –*y* + 1, –*z* + 1
O(W5)···O(52)	3.151			*x*, *y*, *z*
O(W5)···O(W5A)	2.983			–*x* + 1, –*y*, –*z*
O(W5A)···O(41)	2.880			*x*, *y*, *z*
O(W5A)···O(52)	2.897			*x*, *y*, *z*
O(W5A)···O(W5A)	2.964			–*x* + 1, –*y*, –*z*
O(W6)···O(W6)	2.755			–*x* + 1, –*y* + 1, –*z* + 1
O(W6)···O(71)[b]	2.414			*x*, *y*, *z*

[a] A = acceptor; D = donor. [b] These oxygen atoms belong to the acetate counterion.

values for the corresponding bond lengths of other tetranuclear cubane Ni^{II}clusters.[6a,7a,10,14]

There is an amount of hydrogen bonding in **1** (Table 3). The donors are the aqua ligands and the hydroxy groups of all the $(2\text{-py})_2C(OH)O^-$ ligands. A notable feature here is that both uncoordinated and coordinated oxygen atoms of the terminal acetate ligands participate in intracubane hydrogen bonds; of interest is also the fact that the hydroxy oxygen atom O(2) acts both as a donor and an acceptor.

The cation $[Ni_4(O_2CMe)_3\{(2\text{-py})_2C(OH)O\}_4]^+$ present in complex **3**·$2H_2O$·2EtOH also has a cubane structure (Figure 5), with the $\eta^1{:}\eta^3{:}\eta^1\mu_3$ $(2\text{-py})_2C(OH)O^-$ ligands (Figure 3) supplying the O atoms at the alternate sites of the heterocubane. However, its structure is different from the structure of the cation present in **1**. There are no solvate ligands and a third acetate is present. Two acetates are coordinated to each of Ni(2) and Ni(4). The third acetate acts as an 1,3-bridge ($\eta^1{:}\eta^1{:}\mu_2$) between Ni(2) and Ni(4); thus, one face of the cube is capped by the μ_2-bridging acetate which lies across the face diagonally. The metal centers that are bridged by the acetate ion have the shortest metal–metal distance [Ni(2)···Ni(4) 2.970(2) Å]. There are two distinct nickel sites in **3**·$2H_2O$.2EtOH. Two [Ni(1), Ni(3)] have an O_3N_3 coordination sphere, while for the other two [Ni(2),Ni(4)] the coordination environment is O_5N. Three Ni–O (alkoxide-type) distances are realized for Ni(1), Ni(2), and Ni(4). One bond is short with an average of 2.035(6) Å, one bond is relatively long with an average distance of 2.156(7) Å, while the third bond is of intermediate strength [average Ni–O distance of 2.089(7) Å]. For Ni(3) one bond is rather short to a distance of 2.045(7) Å, whereas the two other bonds are longer [2.106(6), 2.100(7) Å]. As in **1**, the $\{Ni_4O_4\}$ cube deviates from the ideal geometry. Since all the hydrogen atoms of this complex were not located by difference maps, we can not comment on the hydrogen bonds.

The molecular structure of the cation $[Ni_4(O_2CMe)_3\{(2\text{-py})_2C(OH)O\}_4]^+$ present in complex **5**·$6H_2O$·MeCN (Figure 6) is almost identical to that of the tetranuclear cation with the same formula in complex **3**·$2H_2O$·2EtOH. Clearly, the replacement of the ClO_4^- counterion by the $MeCO_2^-$ counterion and the change of the lattice solvate molecules have very little structural effect. The crystal structure is stabilized by a series of strong or relatively strong hydrogen bonds with water solvate molecules as donors.

The molecular structure of the cations $[Ni_4(O_2CMe)_3\{(2\text{-py})_2C(OH)O\}_4]^+$ of complexes **3**·$2H_2O$·2EtOH and **5**·$6H_2O$·MeCN is very similar to that of the same cation present in complex $[Ni_4(O_2CMe)_3\{(2\text{-py})_2C(OH)O\}_4](ClO_4)\cdot 8\cdot 25H_2O$.[7a]

Complexes **1**, **3**·$2H_2O$·2EtOH and **5**·$6H_2O$·MeCN join a family of polynuclear Ni^{II} complexes with $(2\text{-py})_2CO$-based ligands, which currently comprises 12 clusters. The eight previously characterized clusters (solvate molecules are not indicated) are $[Ni_9(OH)_2(O_2CMe)_8\{(2\text{-py})_2CO_2\}_4]$,[6f] $[Ni_9(N_3)_2(O_2CMe)_8\{(2\text{-py})_2CO_2\}_4]$,[6f] $[Ni_4(O_2CMe)_3\{(2\text{-py})_2C(OH)O\}_4](ClO_4)$,[7a] $[Ni_4(O_2CMe)_4\{(2\text{-py})_2C(OH)O\}_4]$,[7b] $[Ni_4\{(2\text{-py})_2C(OH)O\}_2\{(2\text{-py})_2C(OEt)O\}_2(CH_3CONHO)_2]Cl_2$,[7b] where CH_3CONHO^- is the acetohydroxamate(–1) ion, $[Ni_4\{N(CN)_2\}_2(O_2CMe)_2\{(2\text{-py})_2C(OH)O\}_4]$,[6a] $\{K[Ni_6(CO_3)(N_3)_6(O_2CMe)_3\{(2\text{-py})_2C(CH_2CN)O\}_3]\}_2[K_2(H_2O)_2]$,[15] where $(2\text{-py})_2C(CH_2CN)O^-$ is the monoanion of a ligand generated in situ by the reaction of MeCN and $(2\text{-py})_2CO$ in the presence of *tert*-butoxide, $[Ni_4(N_3)_4\{(2\text{-py})_2C(OH)O\}_4]$,[9h] and $[Ni_4(N_3)_2\{(2\text{-py})_2C(OH)O\}_2\{(2\text{-py})_2C(OMe)O\}_2(H_2O)_2](ClO_4)_2$.[9i] From the tetranuclear clusters in the above list, only complexes $[Ni_4(O_2CMe)_3\{(2\text{-py})_2C(OH)O\}_4](ClO_4)$,[7a] $[Ni_4\{N(CN)_2\}_2(O_2CMe)_2\{(2\text{-py})_2C(OH)O\}_4]$,[6a] and the clusters **1**, **3**·$2H_2O$·2EtOH, **5**·$6H_2O$·MeCN reported in this work have a cubane structure.

$[Ni_4(O_2CMe)_4\{(2\text{-py})_2C(OH)O\}_4]\cdot 2MeCN$ (4·2MeCN)

A partially labeled plot of the tetranuclear molecule of compound **4** is shown in Figure 7. Selected interatomic dis-

tances and angles are listed in Table 7, while hydrogen bonding details are summarized in Table 8.

Table 7. Selected interatomic distances [Å] and angles [°] for $[Ni_4(O_2CMe)_4\{(2\text{-py})_2C(OH)O\}_4]\cdot 2MeCN$ (**4**·2MeCN).[a]

Ni(1)···Ni(1′)	3.178(1)	Ni(2)–O(1)	2.023(3)
Ni(1)···Ni(2)	3.089(1)	Ni(2)–O(3′)	2.101(3)
Ni(1)···Ni(2′)	3.273(1)	Ni(2)–O(5)	2.025(3)
Ni(2)···Ni(2′)	5.515(1)	Ni(2)–O(11)	2.157(3)
Ni(1)–O(1)	2.108(3)	Ni(2)–N(2)	2.124(4)
Ni(1)–O(3)	2.061(3)	Ni(2)–N(12)	2.089(3)
Ni(1)–O(11)	2.039(3)	C(41)–O(3)	1.303(5)
Ni(1)–O(11′)	2.091(3)	C(41)–O(4)	1.206(6)
Ni(1)–N(1)	2.051(3)	C(43)–O(5)	1.262(5)
Ni(1)–N(11)	2.116(4)	C(43)–O(6)	1.229(6)
O(1)–Ni(1)–O(3)	161.9(1)	Ni(1)–O(1)–Ni(2)	96.8(1)
O(11)–Ni(1)–N(1)	158.6(1)	Ni(1)–O(11)–Ni(2)	94.8(1)
O(11′)–Ni(1)–N(11)	153.2(1)	Ni(1)–O(11)–Ni(1′)	100.6(1)
O(1)–Ni(2)–N(12)	155.8(1)	Ni(1′)–O(11)–Ni(2)	100.8(1)
O(3′)–Ni(2)–N(2)	166.8(1)	Ni(1)–O(3)–Ni(2′)	103.7(1)
O(5)–Ni(2)–O(11)	162.7(1)		

[a] Primed atoms are related to the unprimed ones by the symmetry transformation $-x, -y + 2, -z$.

Table 8. Details for the hydrogen bonding of complex $[Ni_4(O_2CMe)_4\{(2\text{-py})_2C(OH)O\}_4]\cdot 2MeCN$ (**4**·2MeCN).[a]

D–H···A	D···A [Å]	H···A [Å]	DHA [°]	Symmetry operator of A
O(2)–H(O2)···O(6)[b]	2.659	1.992	171.0	x, y, z
O(12)–H(O12)···O(1′)[b]	2.656	1.872	167.7	$-x, -y + 2, -z$

[a] A = acceptor; D = donor. [b] Intramolecular hydrogen bonds.

Complex **4**·2MeCN crystallizes in monoclinic space group $P2_1/n$. Its structure consists of centrosymmetric tetranuclear $[Ni_4(O_2CMe)_4\{(2\text{-py})_2C(OH)_2O\}_4]$ molecules and lattice MeCN molecules; the latter will not be further discussed. The four Ni^{II} ions are located at four vertices of a defect dicubane (two cubanes sharing one face and each missing one vertex, Figure 8) and bridged by means of O atoms from the $(2\text{-py})_2C(OH)O^-$ ligands and two $\eta^2{:}\mu_2$ acetate ions (Figure 9). Peripheral ligation is provided by two O atoms of two monodentate (η^1, Figure 9) acetates and the N atoms of the eight 2-pyridyl rings. Atoms O(11)/O(11′) of two $(2\text{-py})_2C(OH)O^-$ ligands are triply bridging with distances to Ni^{II} ions of 2.039(3), 2.091(3), and 2.157(3) Å. Atoms O(1)/O(1′) of the last two $(2\text{-py})_2C(OH)O^-$ ligands are doubly bridging forming one strong bond to Ni(2)/Ni(2′) [2.023(3) Å] and one weaker bond to Ni(1)/Ni(1′) [2.108(3) Å]. The bridging Ni–$O_{acetate}$ distances [2.061(3), 2.101(3) Å] are slightly asymmetric. The Ni–O bond lengths for the bridging acetate oxygen are longer than the Ni(2)–O(5) distance [2.025(3) Å] exhibited by the terminal acetate. One O atom of each $(2\text{-py})_2C(OH)O^-$ ligand remains protonated and unbound to the metal ions. Therefore, two $(2\text{-py})_2C(OH)O^-$ ligands adopt the $\eta^1{:}\eta^3{:}\eta^1{:}\mu_3$ coordination mode and the other two bind with the $\eta^1{:}\eta^2{:}\eta^1{:}\mu_2$ mode. Ni(1) and Ni(2) are also bridged by the O(3) atom of the $\eta^2{:}\mu_2$ acetate ligand. In the centrosymmetric tetramer two types of octahedrally coordinated Ni^{II} ions can be distinguished, Ni(1) and Ni(2). The two chromophores are Ni(1)(O_{alkoxo})$_3$($O_{acetate}$)N_2 and Ni(2)(O_{alkoxo})$_2$($O_{acetate}$)$_2N_2$.

Complex **4** is the 13th member in the above-mentioned family of structurally characterized Ni^{II} clusters with $(2\text{-py})_2CO$-based ligands.[6a,f,7a,b,9h,i,15] Within this family, complexes **4**, $[Ni_4(O_2CMe)_4\{(2\text{-py})_2C(OH)O\}_4]$ (as the tetraethanol solvate),[7b] $[Ni_4\{(2\text{-py})_2C(OH)O\}_2\{(2\text{-py})_2C(OEt)O\}_2(CH_3CONHO)_2]Cl_2$,[7b] $[Ni_4(N_3)_4\{(2\text{-py})_2C(OH)O\}_4]$,[9h] and $[Ni_4(N_3)_2\{(2\text{-py})_2C(OH)O\}_2\{(2\text{-py})_2C(OMe)O\}_2(H_2O)_2](ClO_4)_2$[9i] have a defect dicubane structural motif. Complex **4** has a remarkable structural similarity with compound $[Ni_4(O_2CMe)_4\{(2\text{-py})_2C(OH)O\}_4]\cdot 4EtOH$;[7b] only the crystal packing of this cluster differs.

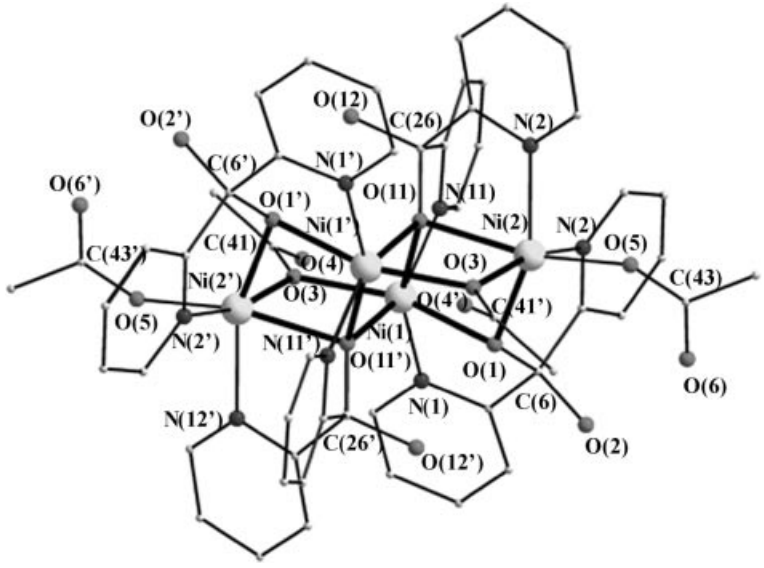

Figure 7. Partially labeled ORTEP plot of the tetranuclear molecule present in complex **4**·2MeCN. Primed and unprimed atoms are related by the crystallographic inversion center. The defect dicubane core has been highlighted.

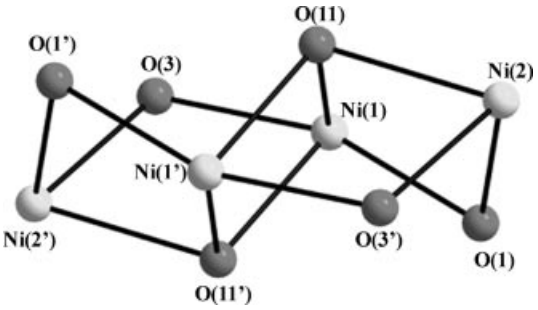

Figure 8. Labeled plot of the defect dicubane core present in complex **4**·2MeCN. Atoms O(3) and O(3′) originate from the η^2:μ_2 acetates, while atoms O(1), O(1′), O(11), and O(11′) are the deprotonated oxygens of the $(2\text{-py})_2C(OH)O^-$ ligands.

Figure 9. The crystallographically established coordination modes of the acetate ligands present in complex **4**·2MeCN.

Tetranuclear Ni^{II} clusters with the defect dicubane unit have been reported,[7b,9h,i,16] but these are significantly less than the Ni^{II} cubanes.

IR Spectra

The prepared complexes exhibit medium to strong intensity bands in the 3605–3150 cm^{-1} region, assignable to ν(OH) vibrations of the $(2\text{-py})_2C(OH)_2$, $(2\text{-py})_2C(OH)O^-$, H_2O, and EtOH ligands/lattice molecules.[6a,9a] The broadness and relatively low frequencies of these bands are both indicative of hydrogen bonding.

The spectrum of **2**·H_2O exhibits a strong band at 1686 cm^{-1}, assigned to ν(C=O) and suggesting that a certain amount of the organic ligand is present in its ketone form. This mode is situated at the same wavenumber (1684 cm^{-1}) in the spectrum of free $(2\text{-py})_2CO$, confirming the nonparticipation of the ketone group in the coordination in this complex. The spectra of **1** and **3**–**5** do not exhibit bands in the region expected for ν(C=O) vibrations, with the nearest IR absorptions at ca. 1600 cm^{-1} assigned as a 2-pyridyl stretching mode raised from 1582 cm^{-1} on coordination, as observed earlier[17] upon complex formation involving hydration of di-2-pyridyl ketone.[17]

Several bands appear in the 1600–1400 cm^{-1} range in the spectra of the complexes. Contributions from the $MeCO_2^-$ $\nu_{as}(CO_2)$ and $\nu_s(CO_2)$ modes would be expected in this region, but overlap with the stretching vibrations of the 2-pyridyl rings and $\delta(CH_3)$ renders assignments tentative and application of the spectroscopic criterion of Deacon and Phillips[18] extremely difficult.

The IR spectra of **1**–**3** exhibit medium or strong bands at ca. 1100 and 620 cm^{-1}, because of the $\nu_3(F_2)$ and $\nu_4(F_2)$ modes of the uncoordinated T_d ClO_4^-, respectively.[19] The $\nu_3(F_2)$ band is broadened and split, indicating the crystallographically established (at least for **1** and **2**) involvement of the ClO_4^- ion in hydrogen bonding.[20]

Magnetic Studies

Solid-state dc magnetic susceptibility measurements were performed on polycrystalline samples of the representative complexes **1** and **4**, under a constant field of 0.5 T in the temperature range of 1.9 to 300 K.

The exchange coupling of four $S = 1$ centers results in $n = 3^4 = 81$ molecular magnetic states that are split into 3 singlets ($S = 0$), 6 triplets ($S = 1$), 6 quintets ($S = 2$), 3 septets ($S = 3$), and 1 nonet ($S = 4$). Depending upon the actual topology, these states can be degenerate (the case of a perfect tetrahedron with a single exchange coupling constant) or the degeneracy can be partially removed.

The structural parameters of **1** suggest a lower symmetry than T_d. The magnetic analyses were carried out using a 2-*J* model and assuming that the tetranuclear structure results from the association of two planar, doubly-bridged dimeric units as shown in Figure 10. The intradimer interaction (noted J_1) is between Ni(1) and Ni(1′) on the one hand and between Ni(2) and Ni(2′) on the other hand, while the interdimer one is noted J_2. The spin Hamiltonian for such a model, reflecting the S_4 symmetry, is given by Equation (7).

$$\hat{H}(\mathbf{S}_4) = -J_1(\vec{S}_1\cdot\vec{S}_{1'} + \vec{S}_2\cdot\vec{S}_{2'}) - J_2(\vec{S}_1\cdot\vec{S}_2 + \vec{S}_1\cdot\vec{S}_{2'} + \vec{S}_{1'}\cdot\vec{S}_2 + \vec{S}_{1'}\cdot\vec{S}_{2'}) + \mu_B B g_{iso}(\vec{S}_1 + \vec{S}_{1'} + \vec{S}_2 + \vec{S}_{2'}) \quad (7)$$

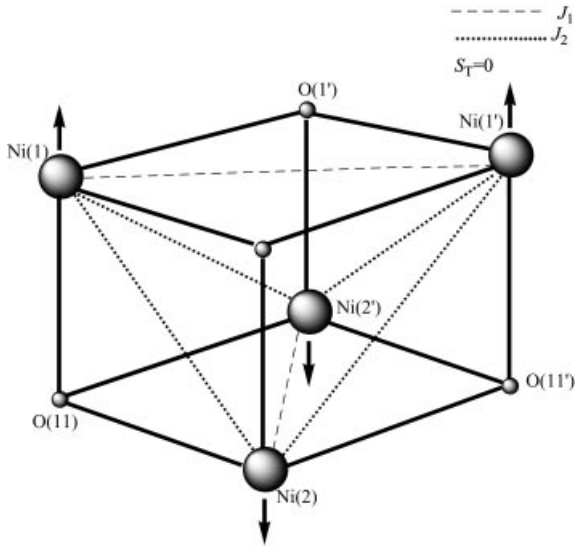

Figure 10. Core representation of the cation of **1** showing the coupling scheme used in the magnetic model and the relative orientation of the Ni^{II} spins in the ground state. The numbering scheme from Figure 4 has been used.

The Hamiltonian matrix in the basis set of coupled kets $|S_1S_{1'}S_{11'}S_2S_{2'}S_{22'}SM\rangle$ is already diagonal, so that the energy levels are given[21] by a simple formula [Equation (8)], where the last, constant term can be omitted.

$$\varepsilon_{B=0}(S) = \left\langle S_{11'}S_{22'}SM \left| \hat{H}(S_4) \right| S_{11'}S_{22'}SM \right\rangle = -(J_2/2)[S(S+1) - S_{11'}(S_{11'}+1) - S_{22'}(S_{22'}+1)] - (J_1/2)[S_{11'}(S_{11'}+1) + S_{22'}(S_{22'}+1)] + (J_1/2)[S_1(S_1+1) + S_{1'}(S_{1'}+1) + S_2(S_2+1) + S_{2'}(S_{2'}+1)] \quad (8)$$

The addition of the Zeeman term results in the formula given by Equation (9), where a single, isotropic g_{iso}-factor common to all magnetic centers occurs.

$$\varepsilon_B(S,M) = \varepsilon_{B=0}(S) + \mu_B g_{iso} MB \quad (9)$$

The identification of the van Vleck coefficients is now an easy task, so that one can applythe van Vleck equation (with a vanishing second-order term) to end up with an analytical formula [Equation (10)] for the mean magnetic susceptibility, where the physical constants in the reduced Curie constant $C_0 = N_A\mu_0\mu_B^2/k$ adopt their usual meaning.

$$\overline{\chi}_{mol} = C_0 \frac{g_{iso}^2}{T} \frac{\sum_S \sum_{M=-S}^{+S} M^2 \exp[-\varepsilon_{B=0}(S)/kT]}{\sum_S \exp[-\varepsilon_{B=0}(S)/kT]} \quad (10)$$

Figure 11 shows plots of the experimental data for **1** in the form of μ_{eff} (effective magnetic moment) per complex, χ_{mol} and χ_{mol}^{-1} vs. T, respectively. The value of μ_{eff} at 300 K is 6.13 μ_B per complex. As the temperature is lowered, μ_{eff} experiences a slight increase, reaching a maximum value of 6.57 μ_B at 30 K, followed by a much sharper decline at lower temperatures, 2.48 μ_B at 1.9 K. The best fit parameters (R = 0.055) are found to be J_1 = 13.7 cm^{-1}, J_2 = –1.4 cm^{-1}, and g_{iso} = 2.14. Since the fit with J constants is sufficient, there is no need to add D to the model, risking an overparameterization. The experimental data show that complex **1** can be described as two ferromagnetically coupled Ni_2 pairs that, in turn, are coupled antiferromagnetically. The zero-field energy levels of **1** are shown in the inset of Figure 11. One can observe that the width of the energy band is less than $\Delta\varepsilon$ <100 cm^{-1}. This means that at ambient temperature a Curie law holds true owing to a uniform population of all energy levels. Upon cooling down, some "magnetically less productive states" (singlets, triplets, quintets) are depopulated and, thus, the overall "magnetic productivity" is raised; under the term "magnetic productivity" we mean the contribution of the state $g^2M^2\exp[\varepsilon_B = {}_0(S)/kT]$ to the susceptibility function and/or the effective magnetic moment. This point explains the maximum of μ_{eff} at 30 K. However, the ground state is S = 0, because of the antiferromagnetic coupling between the two dimeric units. Consequently, the magnetic susceptibility exhibits a turning point on cooling (at 5.0 K), below which it drops to zero. Low-temperature data bring no evidence for the presence of a paramagnetic impurity in **1**. It can not be excluded that the zero-field splitting of the $S \geq 1$ states occurs, as the D values (the axial zero-field splitting parameter), ranging between D/k = –10 and +10 K, are typical for mononuclear Ni^{II} complexes on departure from the octahedral geometry.[22] The involvement of the local anisotropy through the axial zero-field splitting parameter led to a rather slight improvement of the data-fit (R = 0.0082) with magnetic parameters J_1 = 11.7 cm^{-1}, J_2 = –1.3 cm^{-1}, g_{iso} = 2.16, and D_{Ni} = –2.8 cm^{-1}. The obtained D_{Ni} parameter lies at the limit of its detection from the susceptibility data; moreover, it has been obtained by assuming all the D tensors are collinear, the negligible g-tensor anisotropy, and neglect of the pair-interaction $D_{Ni–Ni}$ parameters (the asymmetric exchange) that are inconsistent approximations.[22]

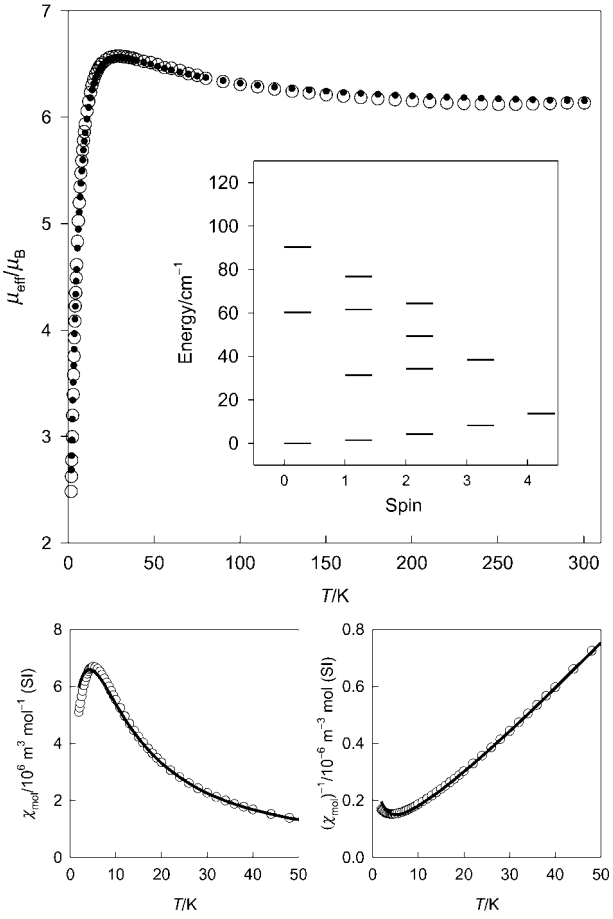

Figure 11. Plots of experimental (open circles) μ_{eff} (left), χ_{mol} (right up) and χ_{mol}^{-1} (right bottom) vs. T per molecule of **1**. The filled circles and the solid lines are the fits to the experimental data (see text for details). Inset: calculated energy levels for individual total spins.

The lowest temperature data (below 5 K) can suffer from eventual saturation effects; when the magnetization approaches saturation, the apparent susceptibility $\chi = \mu_0 M/B$ decreases substantially [the true differential susceptibility, $\tilde{\chi} = \mu_0(\partial M/\partial B)$, as measured by the alternating-current susceptometer, then drops to zero]. Finally, some molecular field correction, accounting for the weak intercluster inter-

actions can contribute to the low-temperature data. All of these effects are assumed to be of secondary importance and they do not alter the main conclusion for **1**, i.e. that the intradimer coupling is of ferromagnetic nature, whereas the interdimer interaction is antiferromagnetic.

It should be mentioned at this point that the most important parameter in the magnetostructural correlation of tetranuclear nickel(II) clusters possessing the $\{Ni_4(\mu_3\text{-}OR)_4\}^{4+}$ cubane core has been reported[6a,10c,14e–h,14k–14n] to be the average Ni–O–Ni angle of a cubane face. A ferromagnetic exchange interaction is observed for Ni–O–Ni angles lower than ca. 99° and the J value increases as the angle decreases. On the other hand, Ni–O–Ni angles in the vicinity of, and larger than, 99° lead to an antiferromagnetic interaction and the $|J|$ value increases as the angle increases. Accordingly, a linear correlation between J and the Ni–O–Ni angle has been reported.[14e] The J_1 and J_2 values for **1** are in line with the previous studies mentioned above. The mean Ni–O–Ni angle for the pairs described by J_1 is 96.6°, thus the coupling is predicted to be ferromagnetic, and indeed, it is (J_1 = 13.7 cm^{-1}). The value of the ferromagnetic parameter J_1 matches satisfactorily the linear dependence reported.[14e,h,l] The mean Ni–O–Ni value of 100.0° for the remaining four faces of the cube justifies the weak antiferromagnetic value of J_2 (–1.4 cm^{-1}).

Magnetically, the closest precedents of complex **1** are the cubanes $[Ni_4(O_2CMe)_3\{(2\text{-py})_2C(OH)O\}_4](ClO_4)$[7a] and $[Ni_4(O_2CCMe_3)_4(Mq)_4]$ (Mq = 1,8-hydroxyquinaldinate);[14n] their behavior was interpreted on the basis of two pairs of ferromagnetically coupled dimers that couple antiferromagnetically to give a diamagnetic ground state.

Variable-temperature magnetic data for complex **4** are presented in Figure 12. As the temperature is lowered, μ_{eff} experiences a very slight increase from μ_{eff} = 5.71 μ_B at 300 K (it practically has a constant value), reaching a broad maximum of μ_{eff} = 5.79 μ_B at 90 K, followed by a much sharper decline at lower temperatures, down to μ_{eff} = 1.33 μ_B at 1.9 K. Considering the cluster topology and core connectivity, the magnetic data were analyzed with the spin Hamiltonian given in Equation (11) [the spin numbering follows the Ni^{II} ions in Figure 8],

$$\hat{H} = -J_1(\vec{S}_1 \cdot \vec{S}_{1'}) - J_2(\vec{S}_1 \cdot \vec{S}_{2'} + \vec{S}_{1'} \cdot \vec{S}_2) - J_3(\vec{S}_1 \cdot \vec{S}_2 + \vec{S}_{1'} \cdot \vec{S}_{2'}) + \mu_B B g_{iso}(\vec{S}_1 + \vec{S}_{1'} + \vec{S}_2 + \vec{S}_{2'}) \quad (11)$$

where J_1 is assigned to the Ni(1)···Ni(1′) interaction of the central pair, J_2 to the Ni(1)···Ni(2′) [Ni(1′)···Ni(2)] interaction, and J_3 to the Ni(1)···Ni(2) [Ni(1′)···Ni(2′)] exchange interaction. The above Hamiltonian cannot be taken to a diagonal form so that we are left with the diagonalization of its matrix elements and a numerical finding of the van Vleck coefficients that enter the formula for the magnetic susceptibility.[23] The best-fit parameters (R = 0.030) are: J_1 = –5.0 cm^{-1}, J_2 = –4.8 cm^{-1}, J_3 = 15.3 cm^{-1} with g = 2.00. The involvement of the local anisotropy through the axial zero-field splitting parameter D_{Ni} led only to a slight improvement of the data-fit (R = 0.018) with magnetic parameters J_1 = –5.3 cm^{-1}, J_2 = –4.6 cm^{-1}, J_3 = 15.7 cm^{-1}, g = 2.00, and D_{Ni} = –2.0 cm^{-1}.

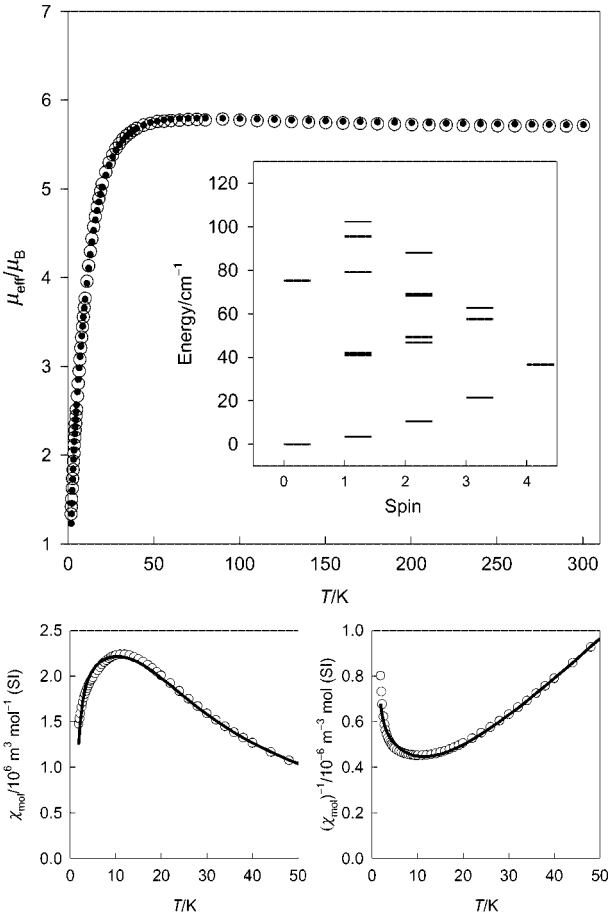

Figure 12. Plots of experimental (open circles) μ_{eff} (left), χ_{mol} (right up) and χ_{mol}^{-1} (right bottom) vs. T per molecule of **4**. The filled circles and the solid lines are the fits to the experimental data (see text for details). Inset: calculated energy levels for individual total spins.

The calculated zero-field, total spin energy levels of complex **4** are shown in the inset of Figure 12. Approaching room temperature, all the levels are equally populated, so that we end up with Curie law behavior. On cooling, however, some magnetically less productive states are depopulated and, thus, the overall magnetic productivity rises. This explains the shallow maximum of μ_{eff} at about 90 K. Upon further cooling below 40 K, the S = 4, S = 3, S = 2, and S = 1 states are gradually depopulated and, therefore, the effective magnetic moment drops to zero. Because of the S = 0 ground state, a turning point exists at 11 K in the χ_{mol} vs. T curve upon cooling.

The signs of the J values are in line with the already mentioned magnetostructural correlation for nickel(II) clusters. The double oxygen bridge [Ni(1)–O(1)–Ni(2) and Ni(1)–O(11)–Ni(2)], which mediates the positive J_3 exchange interaction, has angles of 96.8 and 94.8° that are known to lead to ferromagnetic interactions.[16a] The other two weak antiferromagnetic exchange interactions of –5.0 (J_1) and –4.8 (J_2) are associated with angles in the range

100.6–103.7°; such angles are expected to lead to weak antiferromagnetic interactions.[24] In the three previously characterized[16a,16b] tetranuclear defect dicubane Ni^{II} clusters *possessing exclusively oxygen monoatomic bridges*, ferromagnetic exchange interactions have been observed leading to a $S = 4$ ground state. However, in the present case of **4**, competing ferromagnetic and antiferromagnetic interactions are observed as a result of the two different types of Ni–O–Ni angle values, those at 94.8 and 96.8°, and those between 100.6 and 103.7°. This result further emphasizes the sensitivity of both ferromagnetic and antiferromagnetic exchange interactions with respect to the Ni–O–Ni angles.

Conclusions and Perspectives

The further use of di-2-pyridyl ketone in nickel(II) acetate chemistry has provided access to five new complexes, four tetranuclear and one mononuclear. The structure of **2** is novel in the coordination chemistry of di-2-pyridyl ketone, because this complex constitutes the first example of any metal, in which both the ketone and the *gem*-diol forms coexist as ligands. Complexes **1** and **3**–**5** are valuable additions to the chemistry of tetranuclear Ni^{II} clusters; with their structural characterization, and bearing in mind the relevant literature,[7a,7b] the cubane and the defect dicubane topologies can now be considered as general structural motifs in $Ni^{II}/MeCO_2^-/(2\text{-py})_2CO$ chemistry. For two clusters (**1**, **4**) under investigation we have derived the exchange couplings between Ni^{II} ions. In both cases, the coupling is mediated by the μ-oxygen bridges and one can draw some correlations between the coupling sign and the Ni–O–Ni angles; as has been shown previously, there is a clear trend with ferromagnetic coupling observed for small Ni–O–Ni angles and antiferromagnetic couplings at higher angles. Although **1** and **4** have been found to possess an $S = 0$ ground state, the bridging modes of $(2\text{-py})_2C(OH)O^-$ nevertheless suggest possibilities for other Ni_x species that might exist (e.g. clusters containing SO_4^{2-} instead of $MeCO_2^-$) and that may have high-spin ground states.

Analogues of compounds **1** and **3**–**5** with pivalates or benzoates are not known, at least to date, and it is currently not evident whether the preparation and stability of such cubanes are dependent on the particular nature of the carboxylate ligand. The two terminal acetates present in the structures of **1** and **3**–**5** and the aqua ligands in **1** could have future utility as sites for facile incorporation of other monodentate ligands by metathesis or as a means to access higher-nuclearity species by using bis(monodentate) bridging aromatic heterocycles or α,ω-dicarboxylates. Work is in progress to clarify these matters.

Experimental Section

Materials and Physical Measurements: All manipulations were performed under aerobic conditions using materials and solvents (Merck, Aldrich) as received. Elemental analyses (C, H, N) were performed by the University of Ioannina (Greece) Microanalytical Service using an EA 108 Carlo Erba analyzer. IR spectra (4000–450 cm^{-1}) were recorded with a Perkin–Elmer PC 16 FT-IR spectrometer with samples prepared as KBr pellets. Magnetic susceptibility measurements in the 1.9–300 K range under a field of 0.5 T were performed with a Quantum Design SQUID-based MPMSXL-5-type magnetometer. The magnetometer was calibrated with a palladium rod sample (Materials Research Corporation, measured purity 99.9985%). The measurements were carried out on polycrystalline samples. Data were corrected for diamagnetic contributions using Pascal's constants; the temperature-independent paramagnetism of the Ni^{II} ion was considered to be $Na = 2.5 \cdot 10^{-9}\ m^3\ mol^{-1}$ (SI units).

CAUTION: Although no such tendency was observed during the present work, perchlorate salts are potentially explosive and should be handled with care and in small quantities.

$[Ni_4(O_2CMe)_2\{(2\text{-py})_2C(OH)O\}_4(H_2O)_2](ClO_4)_2$ (1): A solution of $(2\text{-py})_2CO$ (0.100 g, 0.54 mmol) in H_2O (3 mL) was added to an aqueous solution (6 mL) of $Ni(O_2CMe)_2 \cdot 4H_2O$ (0.200 g, 0.80 mmol) and $NaClO_4$ (0.099 g, 0.81 mmol). The resulting green solution was stirred for about 10 min and was then allowed to slowly concentrate by solvent evaporation at room temperature for a period of 8–10 d. Well-formed green needles appeared that were collected by filtration, washed with Me_2CO (2 × 3 mL) and dried in air. Yield (based on the ligand): 0.121 g (64%). $C_{48}H_{46}Cl_2N_8Ni_4O_{22}$ (1392.67): calcd. C 41.39, H 3.34, N 8.05; found C 41.60, H 3.40, N 7.89. Crystals of the product were also obtained by layering the initial aqueous reaction solution with a double volume of Me_2CO (18 mL). IR data (KBr pellet): $\tilde{\nu}$ = 3420 cm^{-1} (s, broad), 3051 (w), 2923 (w), 1604 (s), 1576 (s), 1470 (sh), 1430 (s), 1342 (w), 1290 (w), 1260 (w), 1220 (m), 1122 (s), 1082 (s), 1048 (m), 1022 (sh), 960 (m), 904 (w), 806 (w), 782 (sh), 768 (m), 682 (m), 626 (m), 598 (w), 516 (w), 470 (w) cm^{-1}.

$[Ni(O_2CMe)\{(2\text{-py})_2C(OH)_2\}\{(2\text{-py})_2CO\}](ClO_4) \cdot H_2O$ ($2 \cdot H_2O$): An aqueous, green solution (5 mL) containing $Ni(O_2CMe)_2 \cdot 4H_2O$ (0.062 g, 0.25 mmol) and $NaClO_4$ (0.061 g, 0.50 mmol) were slowly added to a solution of $(2\text{-py})_2CO$ (0.092 g, 0.50 mmol) in H_2O (2.5 mL). A noticeable color change from green to mauve occurred. The resulting mauve solution was stirred for about 10 min and was then allowed to slowly concentrate by solvent evaporation at room temperature for a period of 5–7 d. An approximately 3:1 mixture of brown-red and mauve crystals formed. The crystals were carefully collected by filtration. The two products were readily separable manually, and the brown-red and mauve crystals proved by single-crystal X-ray crystallography to be complexes $2 \cdot H_2O$ and $[Ni\{(2\text{-py})_2C(OH)O\}\{(2\text{-py})_2C(OH)_2\}]_2[Ni\{(2\text{-py})_2C(OH)O\}_2](ClO_4)_2 \cdot 7H_2O$,[11] respectively. Yields for $2 \cdot H_2O$ (based on Ni^{II}) as high as 0.085 g (55%) were obtained. A batch of brown-red crystals was used for analyses and IR spectroscopy. $C_{24}H_{23}ClN_4NiO_{10}$ (621.62): calcd. C 46.40, H 3.74, N 9.02; found C 46.51, H 3.60, N 8.86. IR data (KBr pellet): $\tilde{\nu}$ = 3604 cm^{-1} (m), 3476 (m, broad), 3352 (m, broad), 3082 (w), 3005 (w), 2910 (w), 1686 (s), 1650 (m), 1602 (s), 1574 (m), 1464 (sh), 1442 (s), 1430 (sh), 1318 (s), 1288 (m), 1272 (w), 1232 (m), 1168 (m), 1156 (m), 1104 (s, broad), 1088 (s), 1062 (sh), 1022 (m), 944 (m), 914 (m), 828 (m), 806 (m), 778 (sh), 760 (s), 690 (m), 668 (s), 644 (sh), 624 (s), 576 (m), 512 (w) cm^{-1}.

$[Ni_4(O_2CMe)_3\{(2\text{-py})_2C(OH)O\}_4](ClO_4) \cdot 2H_2O \cdot 2EtOH$ ($3 \cdot 2H_2O \cdot 2EtOH$): A solution of $(2\text{-py})_2CO$ (0.092 g, 0.50 mmol) in EtOH (10 mL) was added dropwise to a slurry of $NaClO_4$ (0.031 g, 0.25 mmol) in the same solvent (15 mL). The obtained slurry was added to a green solution of $Ni(O_2CMe)_2 \cdot 4H_2O$ (0.124 g,

0.50 mmol) in EtOH (20 mL). Solid $NaClO_4$ soon dissolved. The resulting solution was stirred for 45 min at room temperature and allowed to stand undisturbed in a closed flask for 2 d. Well-formed green crystals appeared, which were collected by filtration, washed with ice-cold EtOH (1 mL) and Et_2O (2 × 3 mL) and dried in vacuo with silica gel. Yield (based on Ni^{II}): 0.120 g (71%). The dried solid analyzed as EtOH-free **3**·2H_2O. $C_{50}H_{49}ClN_8Ni_4O_{20}$ (1352.36): calcd. C 44.40, H 3.66, N 8.29; found C 44.51, H 3.49, N 8.25. The obtained crystals were good diffractors of X-rays, as long as they were kept in contact with the mother liquor to prevent EtOH loss. IR data for the dried sample (KBr pellet): $\tilde{\nu}$ = 3425 cm^{-1} (m, broad), 3085 (w, broad), 3017 (w), 2928 (w), 1590 (s, broad), 1443 (sh), 1430 (s), 1341 (w), 1296 (w), 1263 (w), 1218 (m), 1162 (sh), 1082 (s, broad), 1050 (sh), 1012 (sh), 958 (m), 804 (w), 760 (m, broad), 680 (m), 618 (m), 543 (w), 500 (w), 465 (w) cm^{-1}.

$[Ni_4(O_2CMe)_4\{(2\text{-py})_2C(OH)O\}_4]$·2MeCN (4·2MeCN): An almost colorless solution of $(2\text{-py})_2CO$ (0.100 g, 0.54 mmol) in MeCN (10 mL) was added dropwise to a pale green slurry of $Ni(O_2CMe)_2$·4H_2O (0.135 g, 0.54 mmol) in the same solvent (15 mL). The color of the reaction mixture did not change. The mixture was refluxed for 1 h and 45 min, a small quantity of undissolved green material removed by filtration and the filtrate layered with Et_2O (50 mL). Slow mixing gave X-ray quality green crystals of the product. The crystals were collected by filtration, washed with ice-cold MeCN (1 mL) and Et_2O (2 × 2 mL), and dried in vacuo with silica gel. Yield (based on Ni^{II}): 0.128 g (74%). The dried solid analyzed satisfactorily as MeCN-free **4**. $C_{52}H_{48}O_{16}N_8Ni_4$ (1275.92): calcd. C 48.95, H 3.80, N 8.78; found C 48.99, H 3.67, N 8.86. Crystals of the same product could also be isolated, by allowing the initial MeCN solution to slowly evaporate at room temperature. The crystals of **4**·2MeCN were found to lose solvent rapidly, and they were kept in the mother liquor until a suitable crystal had been found for X-ray crystallography. IR data for the dried sample (KBr pellet): $\tilde{\nu}$ = 3418 cm^{-1} (m, broad), 3072 (m), 3025 (w), 2983 (w), 2806 (m, broad), 1638 (sh), 1602 (s), 1574 (s), 1454 (sh), 1438 (sh), 1412 (s), 1370 (m), 1306 (s), 1262 (w), 1210 (s), 1154 (m), 1120 (sh), 1098 (s), 1066 (s), 1046 (sh), 1020 (s), 958 (m), 926 (w), 900 (w), 806 (m), 782 (sh), 764 (s), 684 (s), 656 (s), 640 (sh), 602 (m), 536 (sh), 508 (m), 478 (m) cm^{-1}.

$[Ni_4(O_2CMe)_3\{(2\text{-py})_2C(OH)O\}_4](O_2CMe)$·6$H_2O$·MeCN (5·6$H_2O$·MeCN): EtOH (15 mL) and MeCN (5 mL) were added to a solid mixture containing $Ni(O_2CMe)_2$·4H_2O (0.124 g, 0.50 mmol), $(2\text{-py})_2CO$ (0.092 g, 0.50 mmol), and LiOH·H_2O (0.021 g, 0.50 mmol). Most of the quantities of the solids dissolved upon reflux for 30 min and a cloudy green "solution" was obtained. This was filtered and the solvents were then evaporated under reduced pressure at 35 °C. The obtained residue was dissolved in MeCN (8 mL), filtered and the closed reaction flask containing the filtrate was stored in the refrigerator (ca. 5 °C) for a period of one month. X-ray quality green needles formed, which were collected by filtration, washed with Et_2O (3 mL), and dried in air. Yield (based on Ni^{II}): 0.080 g (46%). The air-dried solid analyzed satisfactorily as MeCN-free **5**·6H_2O. $C_{52}H_{60}O_{22}N_8Ni_4$ (1384.04): calcd. C 45.12, H 4.38, N 8.10; found C 44.91, H 4.41, N 8.02. The crystals of the

Table 9. Crystal data and structure refinement for $[Ni_4(O_2CMe)_2\{(2\text{-py})_2C(OH)O\}_4(H_2O)_2](ClO_4)_2$ (**1**), $[Ni(O_2CMe)\{(2\text{-py})_2C(OH)_2\}\{(2\text{-py})_2CO\}](ClO_4)$·$H_2O$ (**2**·H_2O), and $[Ni_4(O_2CMe)_3\{(2\text{-py})_2C(OH)O\}_4](ClO_4)$·2$H_2O$·2EtOH (**3**·2$H_2O$·2EtOH).

	1	**2**·H_2O	**3**·2H_2O·2EtOH
Empirical formula	$C_{48}H_{46}Cl_2Ni_4N_8O_{22}$	$C_{24}H_{23}ClNiN_4O_{10}$	$C_{54}H_{61}ClNi_4N_8O_{22}$
Mol. mass	1392.67	621.62	1444.40
Color and habit	green needles	brown-red prisms	green prisms
Crystal size [mm]	0.10 × 0.20 × 0.30	0.08 × 0.18 × 0.30	0.08 × 0.40 × 0.55
Crystal system	monoclinic	monoclinic	triclinic
Space group	*C*2/*c*	$P2_1$	$P\bar{1}$
a [Å]	23.258(7)	9.700(1)	11.964(7)
b [Å]	12.097(4)	14.183(1)	13.238(7)
c [Å]	21.312(7)	10.252(1)	19.26(1)
α [°]	90	90	96.37(2)
β [°]	116.97(1)	108.15(1)	93.22(2)
γ [°]	90	90	99.38(2)
V [Å^3]	5344(3)	1340.3(2)	2982(3)
Z	4	2	2
$\rho_{calcd.}$ [g cm^{-3}]	1.731	1.540	1.609
T [°*C*]	25	25	25
λ [Mo-K_a] [Å]	0.71073		0.71073
λ [Cu-K_a] [Å]		1.54180	
μ [mm^{-1}]	1.578	2.523	1.374
F (000)	2848	640	1492
$2\theta_{max}$ [°]	50.00	134.78	44.98
Index ranges	$-27 \le h \le 0$	$0 \le h \le 10$	$-11 \le h \le 11$
	$-14 \le k \le 0$	$-16 \le k \le 13$	$0 \le k \le 14$
	$-21 \le l \le 25$	$-12 \le l \le 11$	$-18 \le l \le 20$
No. of reflections collected	4750	3663	6186
No. of independent reflections/$R_{int.}$	4645/0.0290	3360/0.0205	5861/0.0363
Data with $I > 2\sigma(I)$	3479	3360	4417
Parameters refined	479	462	772
$[\Delta/\sigma]_{max}$	0.029	0.011	0.017
Goodness-of-fit on F^2	1.126	1.061	1.027
$[R_1]$[a]	0.0488	0.0363	0.0711
wR_2[b]	0.1200	0.0994	0.1788
Residuals [e Å^{-3}]	0.918/–0.348	0.409/–0.366	0.936/–0.591

[a] $R_1 = \Sigma(|F_o| - |F_c|)/\Sigma(|F_o|)$. [b] $wR_2 = \{\Sigma[w(F_o^2 - F_c^2)^2]/\Sigma[w(F_o^2)^2]\}1/2$.

product were found to lose MeCN readily, and they were maintained in the mother liquor for X-ray crystallography. IR data for the analytically pure sample (KBr pellet): $\tilde{\nu}$ = 3406 cm^{-1} (m, broad), 3149 (w, broad), 3065 (w, broad), 2925 (w), 2851 (w), 1625 (sh), 1573 (s, broad), 1429 (s, broad), 1402 (m), 1335 (w), 1293 (w), 1215 (m), 1160 (w), 1120 (w), 1080 (m), 1049 (sh), 957 (w), 795 (sh), 770 (m), 675 (m), 660 (sh), 604 (w), 516 (w), 462 (w) cm^{-1}.

X-ray Crystallographic Studies: Crystals of **1**, **3**·2H_2O·2EtOH, **4**·2MeCN, and **5**·6H_2O·MeCN were mounted in capillaries filled with drops of mother liquor, while crystals of **2**·H_2O were stable and mounted in air. Diffraction measurements for **1**, **3**·2H_2O·2EtOH, **4**·2MeCN, and **5**·6H_2O·MeCN were made on a Crystal Logic Dual Goniometer diffractometer using graphite–monochromated M_o-K_α radiation. The X-ray data set for **2**·H_2O was collected with a $P2_1$ Nicolet diffractometer upgraded by Crystal Logic using graphite–monochromated Cu-K_α radiation. Complete crystal data and parameters for data collection and refinement are listed in Table 9 and Table 10. Unit cell dimensions were determined and refined by using the angular settings of 25 automatically centered reflections in the ranges 11° < 2θ < 23° (for **1**, **3**·2H_2O·2EtOH, **4**·2MeCN, and **5**·6H_2O·MeCN) and 22° < 2θ < 54° (for **2**·H_2O). Intensity data were recorded using the θ-2θ scan method. Three standard reflections monitored every 97 reflections showed less than 3% variation and no decay. Lorentz, polarization, and Ψ-scan absorption (for **2**·H_2O, **3**·2H_2O·2EtOH, and **4**·2MeCN) were applied using the Crystal Logic software package. The structures were solved by direct methods using SHELXS-86[25a] and refined by full-matrix least-squares techniques on F^2 with SHELXL-97.[25b] For complexes **2**·H_2O and **3**·2H_2O·2EtOH, the reflections to parameters ratio is relatively low. For the former a full data set was collected for a quarter of the sphere of reflections to 2θ = 135° (for Cu radiation). When the structure was solved it proved to belong to the noncentrosymmetric monoclinic space group $P2_1$. The collection of additional data was continued for a second quarter of the reflections sphere only until 2θ = 95°, because the complex is mononuclear and its structural characterization was valuable mainly in terms of our synthetic efforts. For the latter the data collection was stopped at 2θ = 45° (for Mo radiation), because the molecular structure of the cation present in **3**·2H_2O·2EtOH is almost identical to that of the cation with the same formula in complex **5**·6H_2O·MeCN, for which a full data set to 2θ = 50° had already been collected. For all the structures the ordered non-hydrogen atoms were refined anisotropically. In the case of **1**, the chlorine atoms and one of the perchlorate oxygen atoms were found to be disordered and refined anisotropically over two positions with occupation factors fixed at 0.50. Three of the perchlorate oxygen atoms of **2**·H_2O were found to be disordered and refined in two orientations with occupation factors summing one. In the structure of **3**·2H_2O·2EtOH the solvate molecules were refined isotropically, while the methyl group of one of the acetate ligands was found to be disordered and refined isotropically over two positions with occupation factors summing one. The non-hydrogen atoms of the MeCN solvate molecules of **4**·2MeCN were refined isotropically. For **1**, **2**·H_2O, **4**·2MeCN, and **5**·6H_2O·MeCN, all hydrogen atoms were located by difference maps and were refined isotropically, ex-

Table 10. Crystal data and structure refinement for $[Ni_4(O_2CMe)_4\{(2\text{-py})_2C(OH)O\}_4]$·2MeCN (**4**·2MeCN) and $[Ni_4(O_2CMe)_3\{(2\text{-py})_2C(OH)O\}_4](O_2CMe)$·6$H_2O$·MeCN (**5**·6$H_2O$·MeCN).

	4·2MeCN	**5**·6H_2O·MeCN
Empirical formula	$C_{56}H_{54}Ni_4N_{10}O_{16}$	$C_{54}H_{63}Ni_4N_9O_{22}$
Mol. mass	1357.94	1424.97
Color and habit	greenish prisms	green needles
Crystal size [mm]	0.15×0.25×0.50	0.10×0.20×0.50
Crystal system	monoclinic	triclinic
Space group	$P2_1/n$	$P\bar{1}$
a [Å]	10.343(5)	11.793(4)
b [Å]	12.644(7)	12.863(5)
c [Å]	22.39(1)	20.531(8)
α [°]	90	74.87(2)
β [°]	95.30(2)	85.48(1)
γ [°]	90	79.70(2)
V [Å^3]	2915(3)	2956.3(2)
Z	2	2
$\rho_{calcd.}$ [g cm^{-3}]	1.547	1.601
T [°C]	25	25
λ [Mo-K_a] [Å]	0.71073	0.71073
μ [mm^{-1}]	1.350	1.342
F (000)	1400	1476
$2\theta_{max}$ [°]	50.00	50.00
Index ranges	$-12 \le h \le 0$	$-14 \le h \le 0$
	$-15 \le k \le 0$	$-15 \le k \le 15$
	$-26 \le l \le 26$	$-24 \le l \le 24$
No. of reflections collected	5441	10956
No. of independent reflections/$R_{int.}$	5138/0.0228	10402/0.0110
Data with $I > 2\sigma(I)$	3685	8546
Parameters refined	447	943
$[\Delta/\sigma]_{max}$	0.019	0.014
Goodness-of-fit on F^2	1.052	1.044
$[R_1]$[a]	0.0427	0.0420
wR_2[b]	0.1104	0.1058
Residuals [e Å^{-3}]	0.941/–0.487	0.959/–0.939

[a] $R_1 = \Sigma(|F_o| - |F_c|)/\Sigma(|F_o|)$. [b] $wR_2 = \{\Sigma[w(F_o^2 - F_c^2)^2]/\Sigma[w(F_o^2)^2]\}^{1/2}$.

cept those of the acetate ligands which were introduced at calculated positions as riding on bonded atoms; no hydrogen atoms for the water solvate molecule of **2**·H_2O were included in the refinement. All hydrogen atoms of **3**·2H_2O·2EtOH were introduced at calculated positions as riding on their respective bonded atoms. CCDC-278891, -278892, -278893, -278894, and CCDC-278895 contain the supplementary crystallographic data for this paper. These data can be obtained free of charge from The Cambridge Crystallographic Data Centre via www.ccdc.cam.ac.uk/data_request/cif.

Note Added in Proof (March 22, 2006): After this paper had been submitted, the single-crystal X-ray structure of complex **1** was published. The complex was prepared in MeOH under reflux; however, no magnetic studies for this cluster were reported (Y.-M. Li, J.-J. Zhang, R.-B. Fu, S.-C. Xiang, T.-L. Sheng, D.-Q. Yuan, X.-H. Huang, X.-T. Wu, *Polyhedron*, DOI: 10.1016/j.poly.2005.11.002).

Acknowledgments

S. P. P. thanks the European Social Fund (EST), the Operational Program for Educational and Vocational Training II (EPEAK II), and particularly the Program PYTHAGORAS (Grant b.365.037) for funding of this work. Slovak grant agencies (VEGA 1/2453/05, APVT 20-005204), the Polish Ministry of Science and Computerization, and the 6th Framework Programme EU NoE MAGMANet are also acknowledged.

[1] For excellent reviews, see: a) R. E. P. Winpenny, *Adv. Inorg. Chem.* **2001**, *52*, 1–111; b) R. E. P. Winpenny, *J. Chem. Soc., Dalton Trans.* **2002**, 1–10.

[2] S. Mukhopadhyay, S. K. Mandal, S. Bhaduri, W. H. Armstrong, *Chem. Rev.* **2004**, *104*, 3981–4026.

[3] a) R. Sessoli, H. L. Tsai, A. R. Schake, S. Wang, J. B. Vincent, K. Folting, D. Gatteschi, G. Christou, D. N. Hendrickson, *J. Am. Chem. Soc.* **1993**, *115*, 1804–1816; b) R. Sessoli, D. Gatteschi, A. Caneschi, M. A. Novak, *Nature* **1993**, *365*, 141–143.

[4] For excellent reviews concerning SMMs, see: a) G. Christou, D. Gatteschi, D. N. Hendrickson, R. Sessoli, *MRS Bull.* **2000**, *25*, 66–71; b) D. Gatteschi, R. Sessoli, *Angew. Chem. Int. Ed.* **2003**, *42*, 268–297.

[5] For a comprehensive reference list of 3d-metal SMMs, see: G. Christou, *Polyhedron* **2005**, *24*, 2065–2075.

[6] Recent, representative references from our group: a) G. S. Papaefstathiou, A. Escuer, F. A. Mautner, C. Raptopoulou, A. Terzis, S. P. Perlepes, R. Vicente, *Eur. J. Inorg. Chem.* **2005**, 879–893; b) A. K. Boudalis, B. Donnadieu, V. Nastopoulos, J. M. Clemente-Juan, A. Mari, Y. Sanakis, J.-P. Tuchagues, S. P. Perlepes, *Angew. Chem.* **2004**, *43*, 2266–2270; c) C. J. Milios, E. Kefalloniti, C. P. Raptopoulou, A. Terzis, R. Vicente, N. Lalioti, A. Escuer, S. P. Perlepes, *Chem. Commun.* **2003**, 819–821; d) G. S. Papaefstathiou, A. Escuer, M. Font-Bardia, S. P. Perlepes, X. Solans, R. Vicente, *Polyhedron* **2002**, *21*, 2027–2032; e) N. Lalioti, C. P. Raptopoulou, A. Terzis, A. E. Aliev, I. P. Gerothanassis, E. Manessi-Zoupa, *Angew. Chem. Int. Ed.* **2001**, *40*, 3211–3214; f) G. S. Papaefstathiou, A. Escuer, R. Vicente, M. Font-Bardia, X. Solans, S. P. Perlepes, *Chem. Commun.* **2001**, 2414–2415; g) G. S. Papaefstathiou, S. P. Perlepes, A. Escuer, R. Vicente, M. Fond-Bardia, X. Solans, *Angew. Chem. Int. Ed.* **2001**, *40*, 884–886.

[7] a) M.-L. Tong, S.-L. Zheng, J.-X. Shi, Y.-X. Tong, H. K. Lee, X.-M. Chen, *J. Chem. Soc., Dalton Trans.* **2002**, 1727–1734; b) S. B. Jedner, H. Schwöppe, H. Nimir, A. Rompel, D. A. Brown, B. Krebs, *Inorg. Chim. Acta* **2002**, *340*, 181–186; c) M.-L. Tong, H. K. Lee, Y.-X. Tong, X.-M. Chen, T. C. W. Mak, *Inorg. Chem.* **2000**, *39*, 4666–4669.

[8] For a review, see: G. S. Papaefstathiou, S. P. Perlepes, *Inorg. Chem.* **2002**, *23*, 249–274.

[9] a) E. Katsoulakou, V. Bekiari, C. P. Raptopoulou, A. Terzis, P. Lianos, E. Manessi-Zoupa, S. P. Perlepes, *Spectrochim. Acta Part A* **2005**, *61*, 1627–1638; b) C. Kanaras, B. L. Westcott, G. Crundwell, J. B. Updegraff III, M. Zeller, A. D. Hunter, S. O. Sommerer, *Z. Kristallogr.* **2004**, *219*, 1–2; c) K. N. Crowder, S. J. Garcia, R. L. Burr, J. M. North, M. H. Wilson, B. L. Conley, P. E. Fanwick, P. S. White, K. D. Sienerth, R. M. Granger II, *Inorg. Chem.* **2004**, *43*, 72–78; d) A. K. Boudalis, F. Dahan, A. Bousseksou, J.-P. Tuchagues, S. P. Perlepes, *Dalton Trans.* **2003**, 3411–3418; e) E. Katsoulakou, N. Lalioti, C. P. Raptopoulou, A. Terzis, E. Manessi-Zoupa, S. P. Perlepes, *Inorg. Chem. Commun.* **2002**, *5*, 719–723; f) Z. E. Serna, M. K. Urtiaga, M. G. Barandika, R. Cortés, S. Martin, L. Lezama, M. I. Arriortua, T. Rojo, *Inorg. Chem.* **2001**, *40*, 4550–4555; g) G. S. Papaefstathiou, A. Escuer, C. P. Raptopoulou, A. Terzis, S. P. Perlepes, R. Vicente, *Eur. J. Inorg. Chem.* **2001**, 1567–1574; h) Z. E. Serna, M. G. Barandika, R. Cortés, M. K. Urtiaga, G. E. Barberis, T. Rojo, *J. Chem. Soc., Dalton Trans.* **2000**, 29–34; i) Z. E. Serna, L. Lezama, M. K. Urtiaga, M. I. Arriortua, M. G. Barandika, R. Cortés, T. Rojo, *Angew. Chem. Int. Ed.* **2000**, *39*, 344–347; j) G. Yang, S.-L. Zheng, X.-M. Chen, H. K. Lee, Z.-Y. Zhou, T. C. W. Mak, *Inorg. Chim. Acta* **2000**, *303*, 86–93; k) A. C. Deveson, S. L. Heath, C. J. Harding, A. K. Powell, *J. Chem. Soc., Dalton Trans.* **1996**, 3173–3178; l) A. N. Papadopoulos, V. Tangoulis, C. P. Raptopoulou, A. Terzis, D. P. Kessisoglou, *Inorg. Chem.* **1996**, *35*, 559–565; m) S. R. Breeze, S. Wang, J. E. Greedan, N. P. Raju, *Inorg. Chem.* **1996**, *35*, 6944–6951.

[10] a) E.-C. Yang, W. Wernsdorfer, S. Hill, R. S. Edwards, M. Nakano, S. Maccagnano, L. N. Zakharov, A. L. Rheingold, G. Christou, D. N. Hendrickson, *Polyhedron* **2003**, *22*, 1727–1733; b) R. S. Edwards, S. Maccagnano, E.-C. Yang, S. Hill, W. Wernsdorfer, D. Hendrickson, G. Christou, *J. Appl. Phys.* **2003**, *93*, 7807–7809; c) M. Moragues-Cánovas, M. Helliwell, L. Ricard, E. Riviére, W. Wernsdorfer, E. Brechin, T. Mallah, *Eur. J. Inorg. Chem.* **2004**, 2219–2222.

[11] C. G. Efthymiou, C. P. Raptopoulou, A. Terzis, E. G. Bakalbassis, S. P. Perlepes, manuscript in preparation.

[12] a) V. Tangoulis, C. P. Raptopoulou, S. Paschalidou, E. G. Bakalbassis, S. P. Perlepes, A. Terzis, *Angew. Chem. Int. Ed. Engl.* **1997**, *36*, 1083–1085; b) A. Tsohos, S. Dionyssopoulou, C. P. Raptopoulou, A. Terzis, E. G. Bakalbassis, S. P. Perlepes, *Angew. Chem. Int. Ed.* **1999**, *38*, 983–985.

[13] a) Z. E. Serna, R. Cortés, M. K. Urtiaga, M. G. Barandika, L. Lezama, M. I. Arriortua, T. Rojo, *Eur. J. Inorg. Chem.* **2001**, 865–872; b) J. M. Seco, M. Quirós, M. J. González Garmendia, *Polyhedron* **2000**, *19*, 1005–1013.

[14] a) J. E. Andrew, A. B. Blake, *J. Chem. Soc. A* **1969**, 1556–1560; b) J. A. Bertrand, A. P. Ginsberg, R. I. Kaplan, C. E. Kirkwood, R. L. Martin, R. C. Sherwood, *Inorg. Chem.* **1971**, *10*, 240–246; c) W. Vreugdenhil, J. G. Haasnoot, J. Reedijk, A. L. Spek, *Inorg. Chim. Acta* **1987**, *129*, 205–216, and references cited therein; d) K. S. Murray, *Adv. Inorg. Chem.* **1995**, *43*, 261–358; e) M. A. Halcrow, J.-S. Sun, J. C. Huffman, G. Christou, *Inorg. Chem.* **1995**, *34*, 4167–4177; f) M. S. El Fallah, E. Rentschler, A. Caneschi, D. Gatteschi, *Inorg. Chim. Acta* **1996**, *247*, 231–235; g) A. Escuer, M. Fonta-Bardia, S. B. Kumar, X. Solans, R. Vicente, *Polyhedron* **1999**, *18*, 909–914; h) J. M. Clemente-Juan, B. Chansou, B. Donnadieu, J.-P. Tuchagues, *Inorg. Chem.* **2000**, *39*, 5515–5519; i) A. K. Sah, G. P. Rao, P. K. Saarenketo, K. Rissanen, *Chem. Lett.* **2001**, 1296–1297; j) V. G. Kessler, S. Golih, M. Kritikos, O. N. Korsak, E. E. Knyazeva, I. F. Moskovskaya, B. V. Romanovsky, *Polyhedron* **2001**, *20*, 915–922; k) C. Boskovic, E. Rusanov, H. Stoeckli-Evans, H. U. Güdel, *Inorg. Chem. Commun.* **2002**, *5*, 881–886; l) S. Mukherjee, T. Weyhermüller, E. Bothe, K. Wieghardt, P. Chaudhuri, *Eur. J. Inorg. Chem.* **2003**, 863–875; m) T. K. Paine, E. Rentschler, T. Weyhermüller, P. Chaudhuri, *Eur. J. Inorg. Chem.*

2003, 3167–3178; n) G. Aromi, A. S. Batsanov, P. Christian, M. Helliwell, O. Roubeau, G. A. Timco, R. E. P. Winpenny, *Dalton Trans.* **2003**, 4466–4471; o) G. Chaboussant, R. Basler, H.-U. Güdel, S. Ochsenbein, A. Parkin, S. Parsons, G. Rajaraman, A. Sieber, A. A. Smith, G. A. Timco, R. E. P. Winpenny, *Dalton Trans.* **2004**, 2758–2766; p) A. J. Blake, E. K. Brechin, A. Codron, R. O. Could, C. M. Grant, S. Parsons, J. M. Rawson, R. E. P. Winpenny, *J. Chem. Soc. Chem. Commun.* **1995**, 1983–1985.

[15] M.-L. Tong, M. Monfort, J. M. Clemente Juan, X.-M. Chen, X.-H. Bu, M. Ohba, S. Kitagawa, *Chem. Commun.* **2005**, 233–235.

[16] a) P. King, R. Clérac, W. Wernsdorfer, C. E. Anson, A. K. Powell, *Dalton Trans.* **2004**, 2670–2676; b) J. M. Clemente-Juan, E. Coronado, J. R. Galán-Mascarós, C. J. Gómez-Garzia, *Inorg. Chem.* **1999**, *38*, 55–63; c) T. K. Karmakar, S. K. Chandra, J. Ribas, G. Mostafa, T. H. Lu, B. K. Ghosh, *Chem. Commun.* **2002**, 2364–2365.

[17] P. K. Byers, A. J. Canty, L. M. Engelhardt, J. M. Patrick, A. H. White, *J. Chem. Soc., Dalton Trans.* **1985**, 981–986.

[18] G. B. Deacon, R. J. Phillips, *Coord. Chem. Rev.* **1980**, *33*, 227–250.

[19] K. Nakamoto, *Infrared and Raman Spectra of Inorganic Chemistry and Coordination Compounds*, 4th ed., Wiley, New York, **1986**, pp. 130–138.

[20] G. Christou, S. P. Perlepes, E. Libby, K. Folting, J. C. Huffman, R. J. Webb, D. N. Hendrickson, *Inorg. Chem.* **1990**, *29*, 3657–3666.

[21] R. Boča, *Theoretical Foundations of Molecular Magnetism*, Elsevier, Amsterdam, **1999**.

[22] R. Boča, *Coord. Chem. Rev.* **2004**, *248*, 757–815.

[23] R. Boča, Program *Polymagnet-2002*, Slovak Technical University, Bratislava, **2002**.

[24] S. Wörl, H. Pritzkow, I. O. Fritsky, R. Krämer, *Chem. Commun.* **2005**, 27–29.

[25] a) G. W. Sheldrick, *SHELXS-86*, Program for the Solution of Crystal Structures, University of Göttingen, **1986**; b) G. W. Sheldrick, *SHELXL-97*, Crystal Structure Refinement Program, University of Göttingen, **1997**.

Received: October 7, 2005
Published Online: April 4, 2006

